bioRxiv preprint doi: https://doi.org/10.1101/235853; this version posted December 18, 2017. The copyright holder for this preprint (which was not certified by peer review) is the author/funder. All rights reserved. No reuse allowed without permission.

1 **The ecological genetics of *Pseudomonas syringae* residing on the kiwifruit leaf**
2 **surface**

3 Christina Straub[1], Elena Colombi[1], Li Li[2], Hongwen Huang[2,3], Matthew D. Templeton[4],
4 Honour C. McCann[1 *], Paul B. Rainey[1, 5, 6*]

5 [1] New Zealand Institute for Advanced Study, Massey University, Auckland, New
6 Zealand. [2] Key Laboratory of Plant Germplasm Enhancement and Specialty
7 Agriculture, Wuhan Botanical Garden, Chinese Academy of Sciences, Wuhan, China.
8 [3]Key Laboratory of Plant Resources Conservation and Sustainable Utilization, South
9 China Botanical Garden, Chinese Academy of Sciences, Guangzhou, China. [4]Plant and
10 Food Research, Auckland, New Zealand. [5]Max Planck Institute for Evolutionary
11 Biology, Department of Microbial Population Biology, Plön, Germany. [6] École
12 Supérieure de Physique et de Chimie Industrielles de la Ville de Paris (ESPCI Paris
13 Tech), Laboratoire de Génétique de l'Evolution, Paris, France. * Joint senior authors

14 **CORRESPONDENCE:** Christina Straub, New Zealand Institute for Advanced Study,
15 Massey University, Private Bag 102 904, Auckland 0745, New Zealand. Telephone:
16 +64 9 4140800 ext 43811. e-mail: c.straub@massey.ac.nz

17 **RUNNING TITLE (50 CHARACTERS)**

18 Ecological genetics of *Pseudomonas syringae*

bioRxiv preprint doi: https://doi.org/10.1101/235853; this version posted December 18, 2017. The copyright holder for this preprint (which was not certified by peer review) is the author/funder. All rights reserved. No reuse allowed without permission.

19 **ORIGINALITY-SIGNIFICANT STATEMENT**

20 Bacterial pathogen populations are often studied with little consideration of co-
21 occurring microbes and yet interactions between pathogens and commensals can
22 affect both population structure and disease progression. A fine-scale sampling of
23 commensals present on kiwifruit leaves during an outbreak of bleeding canker
24 disease caused by *P. syringae* pv. *actinidiae* reveals a clonal population structure. A
25 new clade of non-pathogenic *P. syringae* (PG3a) appears to be associated with
26 kiwifruit on a global scale. The presence of PG3a on kiwifruit has significant effects
27 on the outcome of infection by *P. syringae* pv. *actinidiae*. This emphasises the value
28 of studying the effect of co-occurring bacteria on pathogen-plant interactions.

29 **SUMMARY**

30 Interactions between commensal microbes and invading pathogens are
31 understudied, despite their possible impact on pathogen population structure and
32 infection processes. We describe the population structure and genetic diversity of a
33 broad range of co-occurring *Pseudomonas syringae* isolated from infected and
34 uninfected kiwifruit during an outbreak of bleeding canker disease caused by *P.*
35 *syringae* pv. *actinidiae* (*Psa*) in New Zealand. Overall population structure was clonal
36 and affected by ecological factors including infection status and cultivar. Most
37 isolates are members of a new clade in phylogroup 3 (PG3a), also present on
38 kiwifruit leaves in China and Japan. Stability of the polymorphism between
39 pathogenic *Psa* and commensal *P. syringae* PG3a isolates from the same host was
40 tested using reciprocal invasion from rare assays *in vitro* and *in planta*. *P. syringae*

bioRxiv preprint doi: https://doi.org/10.1101/235853; this version posted December 18, 2017. The copyright holder for this preprint (which was not certified by peer review) is the author/funder. All rights reserved. No reuse allowed without permission.

41 G33C (PG3a) inhibited *Psa* NZ54, while the presence of *Psa* NZ54 enhanced the
42 growth of *P. syringae* G33C. This effect could not be attributed to virulence activity
43 encoded by the Type 3 secretion system of *Psa*. Together our data contribute toward
44 the development of an ecological perspective on the genetic structure of pathogen
45 populations.

46 **INTRODUCTION**

47 Kiwifruit (*Actinidia* spp.) cultivation is challenged by outbreaks of the
48 bacterial pathogen *Pseudomonas syringae* pv. *actinidiae (Psa)* – the causative agent
49 of bleeding canker disease. The latest outbreak was first reported in Italy in 2008
50 (Balestra *et al.*, 2008) before spreading rapidly through most kiwifruit growing
51 regions of the world (Abelleira *et al.*, 2011; Everett *et al.*, 2011; Koh *et al.*, 2012;
52 Zhao *et al.*, 2013; Sawada, 2015), arriving in New Zealand in 2010 (Everett *et al.*,
53 2011).

54 As a pathogen, *Psa* faces the challenge of colonising diverse environments
55 before proliferating in the apoplast and vascular tissues. Colonisation of leaf surfaces
56 prior to invasion is a key infection stage (Wilson and Lindow, 1994; Wilson *et al.*,
57 1999; Monier and Lindow, 2003; Pfeilmeier *et al.*, 2016), and *Psa* is likely to
58 encounter and interact with a diverse range of plant-colonising bacteria (Hirano and
59 Upper, 2000; Lindow and Brandl, 2003). Physical proximity increases the likelihood
60 of competitive interactions affecting disease outcomes (Lindow and Brandl, 2003;
61 Hibbing *et al.*, 2010) and increases the probability of horizontal gene transfer
62 (Sawada *et al.*, 1999; Polz *et al.*, 2013; Colombi *et al.*, 2017).

bioRxiv preprint doi: https://doi.org/10.1101/235853; this version posted December 18, 2017. The copyright holder for this preprint (which was not certified by peer review) is the author/funder. All rights reserved. No reuse allowed without permission.

63 Istock *et al.* (1992) made a particularly persuasive case for recognition of and
64 incorporation of local context in the study of bacterial population biology drawing
65 attention to effects on genetic structure (Souza *et al.*, 1992; Haubold and Rainey,
66 1996; Spratt and Maiden, 1999). The impact of studying only focal pathogen
67 populations (Spratt and Maiden, 1999; Cordero *et al.*, 2012; Shapiro *et al.*, 2012;
68 Shapiro and Polz, 2014; Rosen *et al.*, 2015) is particularly apparent in the case of
69 *Neisseria meningitidis* (Maynard Smith *et al.*, 1993; Caugant and Maiden, 2009;
70 Bratcher *et al.*, 2014). Biased sampling of symptomatic *N. meningitidis* produces
71 evidence of linkage disequilibrium, yet the inclusion of *N. meningitidis* from
72 asymptomatic meningococcal infections reveals the population structure of *N.*
73 *meningitidis* to be non-clonal (Maynard Smith *et al.*, 1993; Fraser *et al.*, 2005).

74 Bacterial interactions are context-dependent, ranging from synergistic to
75 antagonistic, and may have both local and global effects on the plant host
76 (Stubbendieck *et al.*, 2016). Antagonistic or competitive interactions between
77 microbes may be direct or indirect, resulting in the inhibition of growth or even
78 killing (Lindow, 1986; Völksch and May, 2001; Berlec, 2012; Hockett *et al.*, 2015;
79 Nakahara *et al.*, 2016). Synergistic interactions occur when multiple types cooperate
80 to cause disease (Singer, 2010; Lamichhane and Venturi, 2015). For example, *P.*
81 *savastanoi* pv. *savastanoi,* causative agent of olive knot disease, interacts with non-
82 pathogenic endophytes *Erwinia sp.* and *Pantoea sp.* in cankers, enhancing the
83 severity of disease (Marchi *et al.*, 2006; Moretti *et al.*, 2011; Buonaurio *et al.*, 2015).
84 Synergistic interactions can also be exploitative: bacteria lacking virulence factors

bioRxiv preprint doi: https://doi.org/10.1101/235853; this version posted December 18, 2017. The copyright holder for this preprint (which was not certified by peer review) is the author/funder. All rights reserved. No reuse allowed without permission.

85 can reap benefits from co-existing pathogenic isolates (Young, 1974; Hirano *et al.*,
86 1999; Macho *et al.*, 2007; Rufián *et al.*, 2017).

87 *P. syringae* is a member of the phyllosphere and engages in both commensal
88 and pathogenic interactions with plants (Hirano and Upper, 2000; Mohr *et al.*, 2008).
89 The diversity and population structure of *P. syringae* has been investigated using
90 both multilocus sequence typing (MLST) and genome sequence analysis of
91 pathogenic isolates collected from diseased plants (Sarkar and Guttman, 2004;
92 Hwang *et al.*, 2005; Baltrus *et al.*, 2011; McCann *et al.*, 2013, 2017; Fujikawa and
93 Sawada, 2016; Nowell *et al.*, 2016), but the broader context of *P. syringae* inhabiting
94 the phyllosphere and its impact on pathogen population structure is largely
95 unknown.

96 Here we describe the population structure of the *P. syringae* species complex
97 inhabiting the kiwifruit phyllosphere during an outbreak of bleeding canker disease
98 in New Zealand. Using an MLST scheme, we reveal a largely clonal population
99 structure, but show that genetic diversity is significantly affected by ecological
100 factors such as infection status and cultivar. We identified members of four *P.*
101 *syringae* phylogroups (PG1, PG2, PG3 and PG5) and recovered a new monophyletic
102 clade within PG3 (PG3a) associated with kiwifruit on a global scale. Investigations
103 into the ecological interactions between a representative of this new clade and *Psa*
104 reveal PG3a inhibits *Psa* proliferation, while *Psa* in turn has a beneficial effect on
105 PG3a growth in kiwifruit.

bioRxiv preprint doi: https://doi.org/10.1101/235853; this version posted December 18, 2017. The copyright holder for this preprint (which was not certified by peer review) is the author/funder. All rights reserved. No reuse allowed without permission.

106 **RESULTS**

107 **Phyllosphere diversity of *Pseudomonas syringae***

108 Four housekeeping genes (*gapA*, *gyrB*, *gltA*, *rpoD*) were sequenced for each
109 of 148 *P. syringae* isolated from two varieties of kiwifruit ('Hayward' and 'Hort16A')
110 in both uninfected and *Psa*-infected orchards. Rarefaction analysis indicates
111 saturation of the sampling effort (Figure S1). The infected 'Hayward' orchard
112 displayed the highest α-diversity (D=0.904), while the uninfected 'Hort16A' orchard
113 displayed the least α-diversity (D=0.737). There was low evenness (ED) among all
114 sampling sites (0.136 to 0.290). Similarly, the four different sampling sites shared
115 few species (Sørensen's index of dissimilarity = 0.847).

116 **Multilocus sequence typing**

117 45 unique sequence types (ST) were discovered among the 148 sequenced
118 strains. All STs were novel, except for ST904 (*Psa*), and not described in the Plant
119 Associated and Environmental Microbes Database (PAMDB). For a more global
120 analysis, *P. syringae* allelic profiles were sourced from PAMDB, Tomihama *et al.*
121 (2016) and Visnovsky *et al.* (2016).

122 Infected orchards (both 'Hayward' and 'Hort16A') harboured the highest
123 number of unique STs, sharing only three STs between them (Figure S2). No STs were
124 present in all four orchards, but two STs were found in three orchards (ST1 and ST3).
125 From the perspective of clonal complexes (CC), the predominant ST (predicted
126 founder) was present along with several SLVs (single locus variants). Two clonal
127 complexes (CC) (21 strains), 5 doubletons (32 strains) and 28 singletons (95 strains)

bioRxiv preprint doi: https://doi.org/10.1101/235853; this version posted December 18, 2017. The copyright holder for this preprint (which was not certified by peer review) is the author/funder. All rights reserved. No reuse allowed without permission.

128 were identified (Figure S3). CC1 and CC2 are comprised of 11 and 10 strains,
129 respectively. ST904 (*Psa*, 15/148) and ST1 (PG3, 24/148) made up 25% of the sample
130 (Figure S3). Strikingly, ST3 (PG3a) was isolated from three out of four orchards and
131 was also sampled from uninfected gold (*A. chinensis* var. *chinensis*) and green (*A.*
132 *chinensis* var. *deliciosa*) kiwifruit in NZ (2010) (Visnovsky *et al.*, 2016) and Japan
133 (2015) (Tomihama *et al.*, 2016), respectively (Figure 1). ST16 was also recovered
134 from uninfected kiwifruit leaves in NZ in both 1991 and 2013. Other Japanese
135 kiwifruit STs group closely with *P. syringae* originating from kiwifruit in NZ.

136 **Sequence diversity**

137 The total concatenated alignment length was 2010 bp with no insertions or
138 deletions detected for either of the four loci. The number of alleles ranged from 25
139 (*gapA*) to 35 (*rpoD*) (Table 1). There were a total of 412 polymorphic sites, ranging
140 from 80 (16.81%, *gapA*) to 145 (28.6%, *gyrB*). The nucleotide diversity index π and
141 Watterson's θ were highly consistent among loci, varying from 0.040 to 0.055 and
142 0.024 to 0.041 respectively. The average GC content of 57.99% is similar to that
143 found in other *P. syringae* studies (59- 61%), however *gyrB* displayed an unusually
144 low GC content of 53.15%. The pairwise genetic difference within phylogroups (PGs)
145 was not greater than 2.7%, whereas among PGs the variability ranged from 6-11%
146 (Table 2), consistent with previous accounts of genetic variability for *P. syringae*
147 (Sarkar and Guttman, 2004; Morris *et al.*, 2010; Berge *et al.*, 2014).

bioRxiv preprint doi: https://doi.org/10.1101/235853; this version posted December 18, 2017. The copyright holder for this preprint (which was not certified by peer review) is the author/funder. All rights reserved. No reuse allowed without permission.

148 **Genetic diversity varies by host cultivar and infection status**

149 To test whether genetic diversity was influenced by the presence of
150 ecological structure, multivariate analyses (PERMANOVA) were performed. A highly
151 significant difference in genetic diversity was observed among sampled orchards
152 (Pseudo-F = 5.99, $P < 0.0001$); with pairwise Permanova tests revealing that the
153 uninfected green orchard differed significantly from every other orchard ($P<0.003$).
154 The cultivar ('Hayward' vs. 'Hort16A') (Pseudo-F = 5.62, $P<0.001$) and infection status
155 of an orchard (Pseudo-F = 11.72, $P<0.001$) also had a significant effect on genetic
156 diversity, whereas no temporal effect was found (Pseudo-F = 1.10, $P>0.34$). When
157 testing the nested effect of all three factors, only the infection status (Pseudo-F =
158 6.42, $P<0.01$) had a significant impact on genetic diversity (Table S3).

159 **Recombination among *P. syringae***

160 Intragenic recombination rates (ρ) ranged from 0.012 (*rpoD*) to 0.038 (*gyrB*)
161 and 0.006 for the concatenated dataset. The ratio ε (recombination rate/mutation
162 rate) ranged from 0.187 (concatenated*)* to 0.931 (*gyrB*) suggesting that any single
163 nucleotide polymorphism is up to five times more likely to have arisen from a
164 mutation than recombination (Table 3).

165 Clustering sequences by PG revealed no evidence of recombination within
166 PG1 and PG5 (ρ=0), however for these phylogroups the sample size was low. There
167 was evidence of recombination in PG3, more specifically for *gltA* (ε=1.18) and *rpoD*
168 (ε=4.07), whereas in PG2 recombination was evident in *rpoD* (ε=1.734) alone. This
169 level of recombination is consistent with earlier reports (Sarkar and Guttman, 2004).

bioRxiv preprint doi: https://doi.org/10.1101/235853; this version posted December 18, 2017. The copyright holder for this preprint (which was not certified by peer review) is the author/funder. All rights reserved. No reuse allowed without permission.

170 Recombination was neither affected by the host cultivar or infection status (Table
171 S4). The analysis was repeated with the inclusion of non-redundant global strains.
172 Overall, intergenic recombination rates were low among PGs, ranging from 0.005 to
173 0.012 for the concatenated dataset (Table S5). In order to pinpoint any effects of
174 recombination on phylogenetic reconstruction, single gene trees were constructed
175 and compared. Tree topologies were significantly different from each other and
176 from the concatenated dataset (SH test, *P*<0.0.5) (Figure S4).

177 **A kiwifruit-associated clade of *P. syringae***

178 Maximum likelihood trees built using the concatenated alignment of unique
179 STs revealed that nearly all NZ *P. syringae* kiwifruit isolates fell within four PGs: PG1
180 (13%), PG2 (29%) and PG3 (56%), with only a few isolates falling into PG5 (2%, Figure
181 2). Strikingly, within PG3 all NZ kiwifruit-associated isolates grouped within a new
182 clade of PG3, hereafter referred to as PG3a. The uninfected orchards showed a
183 higher number of PG3a isolates compared to infected orchards, although no
184 influence of infection status was reflected in the number of unique sequence types
185 (Table S1). This new subclade of PG3 was briefly described from a small-scale
186 sampling of Japanese kiwifruit (clade KID0001, Tomihama *et al*. 2016). We also found
187 that two strains isolated from kiwifruit in NZ in 2010 and 2011 (Visnovsky *et al.*,
188 2016) belong to this subclade.

189 This discovery led us to question whether the PG3a subclade might be prevalent on
190 kiwifruit vines in other countries. To this end we interrogated an unpublished set of
191 *P. syringae* strains collected from kiwifruit leaves in China (sampling as described in
192 McCann *et al.* (2017), GenBank accession numbers: MG674624 – MG674645). A

bioRxiv preprint doi: https://doi.org/10.1101/235853; this version posted December 18, 2017. The copyright holder for this preprint (which was not certified by peer review) is the author/funder. All rights reserved. No reuse allowed without permission.

193 phylogenetic tree based on *gltA* for NZ, Japanese and Chinese kiwifruit isolates
194 revealed that isolates obtained from Chinese kiwifruit also clustered within PG3a
195 (Figure 3). Interestingly, included in this group is isolate 47L9, which was collected
196 from tea leaves (*Camellia* sp.) growing in a former kiwifruit orchard in China. No
197 other *P. syringae* strain from the PAMDB database grouped with PG3a, suggesting
198 PG3a is persistently associated with kiwifruit on a global scale.

199 **Ecological interactions between PG3a and PG1**

200 To assess whether kiwifruit-associated PG3a strains are stably maintained
201 with *Psa* (PG1), co-inoculation experiments were performed *in vitro* and *in planta*.
202 Two isolates sampled from the same leaf were chosen for these experiments as they
203 were isolated from the same leaf: *P. syringae* G33C (ST1, PG3a) and *Psa* NZ54
204 (ST904, PG1).

205 **In vitro *dynamics***

206 *Psa* NZ54 and *P. syringae* G33C showed similar growth dynamics when grown
207 individually *in vitro* (Figure 4). However, when co-inoculated in liquid King's B (KB)
208 media at an equal starting ratio, *Psa* NZ54 growth was significantly reduced (up to
209 100-fold) at 24 h (P <0.001, paired t-tests). This effect was amplified in shaken liquid
210 minimal M9 medium, which mimics the nutrient-poor conditions encountered on
211 the leaf surface (Hernández-Morales *et al.*, 2009): *Psa* NZ54 population density
212 collapsed by 20 h in shaken M9 media (relative fitness -12.1 ±0.09, Figure 4).

213 In order to establish whether the instability of the interaction was influenced
214 by the ratio of founder cells, we investigated whether *P. syringae* G33C could invade

bioRxiv preprint doi: https://doi.org/10.1101/235853; this version posted December 18, 2017. The copyright holder for this preprint (which was not certified by peer review) is the author/funder. All rights reserved. No reuse allowed without permission.

215 from rare initial frequency. *P. syringae* G33C successfully invaded from rare after
216 only 24 h in both rich KB and minimal M9 media (10:1 *Psa NZ54* : *P. syringae* G33C)
217 and reached a similar population size as when cultured on its own in M9 (Figure 5A).
218 Conversely, *Psa* NZ54 also invaded *P. syringae* G33C from rare (*1:10 Psa* NZ54 : *P.*
219 *syringae* G33C), though it established a 100-fold reduced population size of 10^5 - 10^6
220 cfu ml^{-1} compared to growth alone. The population collapse of *Psa* NZ54 in shaken
221 M9, as observed for the 1:1 competition experiments, was once again observed
222 (Figure 5B). The striking suppression of *Psa* NZ54 by *P. syringae* G33C was
223 unambiguously repeated across three experiments. *P. syringae* G33C outcompetes
224 *Psa* NZ54, though both isolates can invade from rare *in vitro* (with the exception of
225 *Psa* NZ54 in shaken M9), which suggests that in a controlled environment the
226 polymorphism is stable.

227 **In planta *dynamics***

228 *In planta* experiments were performed on two gold cultivars, 'Hort16A' and
229 'SunGold', to determine whether *Psa* NZ54 and *P. syringae* G33C also form a stable
230 polymorphism on kiwifruit leaves. *P. syringae* G33C established an epiphytic and
231 endophytic population size in both cultivars (Figure 6) and did not produce any
232 visible symptoms in 'Hort16A' and 'SunGold' (Figure S5, Figure S6). *Psa* NZ54
233 attained a population size at least 10,000-fold greater than *P. syringae* G33C in both
234 hosts. However, endophytic and epiphytic growth were reduced 10-fold in 'SunGold'
235 compared to 'Hort16A' (*P* <0.05, Mann-Whitney U test). Plants inoculated with *Psa*
236 NZ54 developed the first leaf spots at 4 dpi and exhibited severe symptoms at 7 dpi

bioRxiv preprint doi: https://doi.org/10.1101/235853; this version posted December 18, 2017. The copyright holder for this preprint (which was not certified by peer review) is the author/funder. All rights reserved. No reuse allowed without permission.

237 in the more susceptible 'Hort16A', whereas in 'SunGold' leaves displayed only minor
238 symptoms at 7 dpi.

239 In 1:1 competition experiments non-pathogenic *P. syringae* G33C maintained
240 a stable population size. The presence of *Psa* NZ54 had a highly significant positive
241 effect on the growth of *P. syringae* G33C in both plant hosts (Figure 6A&B). *P.*
242 *syringae* G33C established up to 1000-fold higher epiphytic population densities in
243 'Hort16A' (P <0.01, paired t-tests) and 10-fold higher epiphytic and endophytic
244 population densities in 'SunGold' plants (P <0.05, paired t-test) compared to its
245 individual growth. Co-inoculated *Psa* NZ54 exhibited a significant reduction (P <0.05,
246 paired t-test) in epiphytic and endophytic growth on 'Hort16A' in the presence of *P.*
247 *syringae* G33C, but only in the early stages of the experiment. On 'SunGold' the
248 diminished growth of *Psa* NZ54 was more pronounced, with a 100-fold decrease for
249 the endophytic population at 7 dpi (P <0.05, paired t-test, Figure 6B). Co-inoculated
250 'Hort16A' plants exhibited a notable delay in symptom onset compared to singly
251 inoculated plants (Figure S5), whereas there was no difference for 'SunGold' (Figure
252 S6). The increased fitness of *Psa* NZ54 relative to *P. syringae* G33C in 'Hort16A'
253 competition experiments was reflected in the relative fitness parameters (0.7± 0.1*
254 for epiphytic and 4.9± 0.8* for endophytic, * P <0.05, t-test), whereas in 'SunGold'
255 plants *P. syringae* G33C performed better in the epiphytic environment (-1.6 ± 0.2;
256 4.7 ± 0.1* for endophytic growth).

257 To assess whether the heightened growth of *P. syringae* G33C in the
258 presence of *Psa* NZ54 was due to the virulence activity of the pathogen elicited by
259 the Type 3 Secretion System (T3SS), the competition experiment was performed

bioRxiv preprint doi: https://doi.org/10.1101/235853; this version posted December 18, 2017. The copyright holder for this preprint (which was not certified by peer review) is the author/funder. All rights reserved. No reuse allowed without permission.

260 using a T3SS deficient mutant (*Psa* NZ13 Δ*hrcC*). Epiphytic growth of *P. syringae*
261 G33C on 'SunGold' remained elevated when co-inoculated with *Psa* NZ13 Δ*hrcC*,
262 indicating the virulence activity encoded by the T3SS was not responsible for the
263 advantage conferred to the non-pathogenic strain ($P < 0.05$, paired *t*-test, Figure 6C).

264 A rarity threshold for *P. syringae* G33C determines the ability to establish a stable
265 population *in planta*. Upon co-inoculation in a 100:1 (*Psa* NZ54 : *P. syringae* G33C)
266 ratio on 'Hort16A', *P. syringae* G33C was able to invade from rare over the first 4
267 days, but was then excluded by *Psa* NZ54 (Figure 7B). An initial increase in growth of
268 *P. syringae* G33C from 0 dpi to 4 dpi was followed by a population collapse at 7 dpi
269 with no endophytic growth detected and minimal epiphytic growth in environments
270 dominated by *Psa* NZ54. Conversely, *Psa* NZ54 grew to the same population size in
271 the presence of *P. syringae* G33C, as when inoculated individually ($P > 0.1$, paired *t*-
272 tests).

273 In the reciprocal experiment (1:100 *Psa* NZ54 : *P. syringae* G33C), *Psa* NZ54
274 successfully invaded from rare in both the endophytic and epiphytic environment,
275 although the rate of invasion was reduced on the leaf surface . However, both epi-
276 and endophytic population sizes were significantly reduced compared to single
277 inoculations ($P < 0.01$, paired *t*-tests) (Figure 7). Despite the growing population of
278 *Psa* NZ54, *P. syringae* G33C maintained the same epiphytic population size as when
279 inoculated individually ($P > 0.2$, paired *t*-tests). The endophytic population size of *P.*
280 *syringae* G33C increased ($P < 0.01$, 7dpi, paired *t*-test), which mirrored the results
281 from the 1:1 competition experiments, where the presence of *Psa* NZ54 also had a
282 positive effect on growth of *P. syringae* G33C.

bioRxiv preprint doi: https://doi.org/10.1101/235853; this version posted December 18, 2017. The copyright holder for this preprint (which was not certified by peer review) is the author/funder. All rights reserved. No reuse allowed without permission.

283 In order to establish whether there was an advantage to being an early
284 colonist, a time-stagger experiment was performed to see whether immigration
285 history influences the interaction (Fukami *et al.*, 2007). 'Hort16A' plants were pre-
286 inoculated with either of the two strains and followed by a subsequent inoculation
287 of the other strain after three days. Early colonization provided no advantage to *Psa*
288 NZ54 (Figure 8A), as *P. syringae* G33C maintained and established a stable
289 population by 7 dpi and exhibited no significant difference in growth compared to
290 individual growth ($P > 0.3$, paired *t*-tests). Reducing the secondary inoculation density
291 resulted in a reduced initial population size at 3 and 7 dpi for *P. syringae* G33C (P
292 < 0.05, paired *t*-tests), but by 10 dpi the level was the same as when the two strains
293 were grown individually (Figure S7C).

294 When *P. syringae* G33C was the first colonist (Figure 8B) *Psa* NZ54 grew to
295 the same population size by 7 dpi as compared to individually inoculated plants (P
296 > 0.5, paired *t*-tests). The growth of *Psa* NZ54 was initially lower compared to
297 individual growth when inoculated at a lower density ($P < 0.05$, paired *t*-tests), but
298 this difference was no longer evident for the epiphytic population by 10 dpi (Figure
299 S7B).

300 **DISCUSSION**

301 Studies of pathogen populations rarely take into consideration co-occurring
302 commensal types and yet such types are likely to be important contributors to
303 population structure and infection progress (Lindow and Brandl, 2003; Demba Diallo
304 *et al.*, 2012; Bartoli *et al.*, 2015; Buonaurio *et al.*, 2015; Rufián *et al.*, 2017). Here,

bioRxiv preprint doi: https://doi.org/10.1101/235853; this version posted December 18, 2017. The copyright holder for this preprint (which was not certified by peer review) is the author/funder. All rights reserved. No reuse allowed without permission.

305 with focus on *P. syringae*, we have combined traditional population genetic
306 approaches with experiments designed to investigate interactions among members
307 of an ecologically cohesive population. The most significant findings include (i) a
308 clonal population structure for commensal kiwifruit *P. syringae* (ii) strong association
309 of genetic diversity with ecological factors, (iii) discovery of a new clade of kiwifruit-
310 associated kiwifruit *P. syringae* within PG3 (PG3a) (Figure 2, Figure 3), (iv) complex
311 interactions between the pathogenic *Psa* isolate and PG3a with evidence of a stable
312 polymorphism under some *in vitro* conditions, but not *in planta* (Figure 4, Figure 6).

313 Overall, we found that *P. syringae* from kiwifruit display a clonal population
314 structure, comprised of two clonal complexes and a small number of abundant STs.
315 This sits in accord with earlier reports of clonal population structure for *P. syringae*,
316 despite focus on pathogenic isolates which tend to undergo clonal expansion upon
317 host specialisation (Sarkar and Guttman, 2004). Homologous recombination events
318 are few and limited to within phylogroups for *P. syringae*, which is also supported by
319 well-defined phylogenetic clades (Baltrus *et al.*, 2011; Bull *et al.*, 2011; Berge *et al.*,
320 2014; Nowell *et al.*, 2016). A more fine-scale analysis of a collection of *Pseudomonas*
321 *viridiflava* (now *P. syringae* PG7 and PG8 (Bartoli *et al.*, 2014; Berge *et al.*, 2014))
322 isolated from *Arabidopsis thaliana* suggests that recombination at the phylogroup
323 level is primarily within-clade rather than between clade (Goss *et al.*, 2005).

324 Genetic diversity varied according to ecological factors, most strikingly for *P.*
325 *syringae* collected from infected orchards, where genetic diversity was highest. This
326 may reflect effects of *Psa* on the kiwifruit immune response, which may facilitate
327 migration of leaf colonists into the apoplast and vascular tissues and thus allow

bioRxiv preprint doi: https://doi.org/10.1101/235853; this version posted December 18, 2017. The copyright holder for this preprint (which was not certified by peer review) is the author/funder. All rights reserved. No reuse allowed without permission.

328 access to water and nutrients. Such effects have been reported for infection of
329 potatoes by *Pectobacterium atrosepticum* (Kõiv *et al.*, 2015) and herbivore-damaged
330 bitter cress leaves (*Cardamine cordifolia*) (Humphrey *et al.*, 2014), where in both
331 instances *Pseudomonas* population densities and diversity increased following plant
332 damage.

333 We observed differences in *P. syringae* genetic diversity that appear to be
334 attributable to differences in plant genotypes. Host species and cultivar identity is
335 known to significantly affect the composition of phyllosphere bacterial communities
336 (Adams and Kloepper, 2002; Van Overbeek and Van Elsas, 2008; Whipps *et al.*, 2008;
337 Bodenhausen *et al.*, 2014; Laforest-Lapointe *et al.*, 2016; Wagner *et al.*, 2016).
338 Differences in phyllosphere *P. syringae* diversity may also be influenced by
339 environmental factors (such as humidity, nutrient availability or UV radiation) and
340 orchard management practices. Different fertilizer and spray regimes (copper,
341 antibiotics, Actigard™ and biological agents) are employed by growers to prevent or
342 manage *Psa* infection throughout the growing season
343 (http://www.kvh.org.nz/vdb/document/99346). These practices may have selected
344 for copper and streptomycin resistance in *Psa* and kiwifruit epiphytes in NZ and
345 elsewhere (Han *et al.*, 2003; Colombi *et al.*, 2017; Petriccione *et al.*, 2017).

346 Strains grouping with four major phylogroups (PG1, PG2, PG3, PG5) were
347 recovered. This level of diversity in a cultivated environment is not surprising (Goss
348 *et al.*, 2005; Bull *et al.*, 2011; Kniskern *et al.*, 2011; Beiki *et al.*, 2016; Hall *et al.*,
349 2016). Two clades of endophytic *P. syringae* pv. *syringae* were recovered from
350 symptomatic grapevines in Australia with pathogenic and non-pathogenic isolates

bioRxiv preprint doi: https://doi.org/10.1101/235853; this version posted December 18, 2017. The copyright holder for this preprint (which was not certified by peer review) is the author/funder. All rights reserved. No reuse allowed without permission.

351 clustering together (Hall *et al.*, 2016). Samples obtained from citrus orchards
352 suffering from citrus blast caused by *P. syringae* pv. *syringae* revealed isolates
353 associated with PG2, PG7 and an unknown clade (Beiki *et al.*, 2016). Two distinct and
354 highly divergent subclades of *Pseudomonas viridiflava* (*P. syringae* PG7) were
355 recovered from a global sampling of wild *A. thaliana* (Goss *et al.*, 2005).

356 The newly recognised PG3a subclade of *P. syringae* appear to colonise
357 kiwifruit leaves not only in NZ (dating back to 2010 (Visnovsky *et al.*, 2016)), but also
358 in other kiwifruit growing regions of the world, including Japan (Tomihama *et al.*,
359 2016) and China. Data from leaf samples indicate that PG3a is not displaced by *Psa*,
360 but the total number of PG3a isolates collected is reduced in infected orchards.
361 Interestingly the diversity of PG3a does not seem to be affected by infection status.
362 Strains clustering with PG3a formed the majority (>50%) of kiwifruit isolates, and
363 these have not yet been isolated from any other plant hosts recorded in PAMDB,
364 with the exception of isolate 47L9, collected from tea leaves (*Camellia* sp.) growing
365 in a former kiwifruit orchard. This indicates that PG3a forms a persistent association
366 with kiwifruit plants – an observation that is further supported by the repeated
367 isolation of PG3a from kiwifruit across large geographic distances, suggests that
368 PG3a may have been coevolving with its host for some time. PG3a is thus also likely
369 to be disseminated with the exchange of plant material (such as pollen or plant
370 cuttings) between kiwifruit growing countries. The prevalence of PG3a in other
371 kiwifruit growing countries (e.g. Korea, France or Italy) is at present unknown. The
372 preferential occurrence of PG3 with woody hosts (Bartoli *et al.*, 2015; Nowell *et al.*,
373 2016) could explain the particular grouping of the kiwifruit resident clade within

bioRxiv preprint doi: https://doi.org/10.1101/235853; this version posted December 18, 2017. The copyright holder for this preprint (which was not certified by peer review) is the author/funder. All rights reserved. No reuse allowed without permission.

374 PG3. A similarly intriguing signal of host association was found in a collection of *P.*
375 *syringae* isolates from *A. thaliana*, where PG2 representatives dominated (Kniskern
376 *et al.*, 2011; Karasov *et al.*, 2017). Distinct lineages of non-pathogenic isolates have
377 also been described for other plant pathogens such as *Xanthomonas arboricola,*
378 where non-pathogenic strains are distant relatives of pathogenic lineages, despite
379 being isolated from the same host (Essakhi *et al.*, 2015; Triplett *et al.*, 2015).

380 The kiwifruit commensal *P. syringae* G33C (representative of the PG3a
381 subclade) successfully colonized the leaf surface and apoplast of kiwifruit without
382 production of visible disease symptoms. This is reflected in the population size,
383 which was reduced by 4-logs compared to pathogenic population size of *Psa* at 3 dpi.
384 Similar population sizes have been reported for *P. syringae* pv. *phaseolicola*, which
385 grows to a four-log higher population size on its host plant *Phaseolus vulgaris*
386 compared to a non-pathogenic isolate; a 4-log reduction was also observed in
387 resistant vs susceptible hosts (Omer and Wood, 1969; Young, 1974). Similar
388 observations have been made for other plant pathogens, for example non-
389 pathogenic *Xanthomonas* sp. displays a 4-log reduced growth compared to the
390 disease-causing *X. oryzae* pv. *oryzae* (Triplett *et al.*, 2015). Bacterial population
391 density appears to be directly related to the production of disease symptoms, as was
392 demonstrated for environmental *P. syringae* strains inoculated in kiwifruit, which
393 grew to near pathogen population size levels, but induced symptoms of disease
394 (Bartoli *et al.*, 2015).

395 When grown in competition with *Psa* NZ54, *P. syringae* G33C population
396 size increased. Studies exploring the dynamics of mixed infections have

bioRxiv preprint doi: https://doi.org/10.1101/235853; this version posted December 18, 2017. The copyright holder for this preprint (which was not certified by peer review) is the author/funder. All rights reserved. No reuse allowed without permission.

397 demonstrated inoculum density-dependent effects on colonization (Young, 1974;
398 Macho *et al.*, 2007). The ability of non-pathogenic *P. syringae* to colonize wider
399 territories in the presence of a pathogenic strain was nicely demonstrated in a
400 confocal microscopy study (Rufián *et al.*, 2017). It is possible that *P. syringae* G33C
401 benefits from the virulence activity of *Psa* NZ54. T3SS-dependent hitch-hiking effects
402 have been observed for *P. syringae* pv. *syringae* (Hirano *et al.*, 1999), however the
403 increase *in P.* syringae G33C growth persists even in the absence of a functional T3SS
404 in the pathogenic *Psa* strain. Virulence activities not encoded by the T3SS, such as
405 phytotoxin production, may be responsible for this outcome.

406 Epiphytic and *in vitro* growth of *Psa* NZ54 was significantly reduced when
407 co-inoculated with *P. syringae* G33C. Similarly, *Psa* growth may be suppressed by co-
408 inoculation with environmental isolates of *P. syringae* (Bartoli *et al.*, 2015). Epiphytes
409 may suppress pathogen growth either as direct antagonists or indirectly via resource
410 competition (Wilson and Lindow, 1994). The specific mechanism by which *P.*
411 *syringae* G33C suppresses *Psa* remains undetermined. The *Psa* NZ54 population
412 collapse was delayed at 1:10 and 10:1 inoculation ratios, which suggests that this
413 effect was due to the accumulation of antimicrobial compounds produced by *P.*
414 *syringae* G33C. Phytotoxin production is widespread among fluorescent
415 pseudomonads and some toxins have antimicrobial activity (Bender *et al.*, 1999),
416 though contact-dependant growth inhibition (CDI) via Type 5 and 6 secretion
417 systems or bacteriocins may also mediate *P. syringae* interactions (Hayes *et al.*,
418 2010; Haapalainen *et al.*, 2012; Ruhe *et al.*, 2013; Hockett *et al.*, 2015).

bioRxiv preprint doi: https://doi.org/10.1101/235853; this version posted December 18, 2017. The copyright holder for this preprint (which was not certified by peer review) is the author/funder. All rights reserved. No reuse allowed without permission.

419 Our in-depth localised sampling has revealed a global association of PG3a
420 with kiwifruit. Additionally we have shown that this clade of non-pathogenic *P.*
421 *syringae* engage in complex interactions with pathogenic *Psa*. This highlights the
422 value of understanding genotypic diversity and ecological interactions among
423 pathogens and non-pathogens in field settings. Clarifying how commensals persist in
424 association with specific hosts over long periods without causing disease and the
425 mechanism by which they modulate pathogen invasion and proliferation will
426 contribute to a fuller understanding of plant-microbe interactions.

427 **EXPERIMENTAL PROCEDURES**

428 **Plant tissue collection and bacterial isolation**

429 The sampling scheme was designed to obtain strains from *Psa* infected and
430 uninfected hosts, irrespective of disease stage (symptom development) or
431 pathogenicity potential of the isolate. *P. syringae* was isolated from the leaf surfaces
432 of two different cultivars of *Actinidia chinensis*: *A. chinensis* var. *chinensis* Hort16A
433 (gold) and *A. chinensis* var. *deliciosa* Hayward (green), which vary in their
434 susceptibility to *Psa*: 'Hort16A' is more susceptible than the green 'Hayward'
435 (Ferrante and Scortichini, 2010; Cameron and Sarojini, 2014). One infected and one
436 uninfected orchard of each variety was sampled by collecting three leaves from six
437 separate vines along a diagonal path of ~400m (Table S1). Sampling occurred at
438 three intervals during the growing season: spring (after bud break), summer and
439 autumn (prior to harvest). Vine trunks and canes (secondary branches) were tagged
440 to ensure resampling of the same spot. Some 'Hort16A' canes were removed during

bioRxiv preprint doi: https://doi.org/10.1101/235853; this version posted December 18, 2017. The copyright holder for this preprint (which was not certified by peer review) is the author/funder. All rights reserved. No reuse allowed without permission.

441 routine disease management; neighbouring canes on the same vine were then
442 sampled and tagged. All uninfected Hayward vines were cut down prior to the last
443 sampling day so the adjoining block of Hayward was sampled instead. The location of
444 each sampled orchard is listed in Table S2.

445 Leaves were individually placed in 50 mL conical centrifuge tubes and washed
446 with 40 mL 10mM $MgSO_4$ buffer supplemented with 0.2 % Tween (Invitrogen, US) by
447 alternately shaking and vortexing at slow speed for 3 min. After removing the leaf,
448 the leaf wash was centrifuged at 4600 rpm for 10 min. The supernatant was
449 removed and the pellet was resuspended in 200 µL 10mM $MgSO_4$. 100 µL of the
450 resuspension was stored at -80°C and 100 µL was plated on *Pseudomonas* agar base
451 (Oxoid, UK) supplemented with 10 mg/L cetrimide, 10 mg/L fucidin and 50 mg/L
452 cephalosporin (CFC supplement, Oxoid, UK). For each leaf two isolates exhibiting *P.*
453 *syringae* colony morphology (round, creamy white) were selected randomly from
454 the plate and restreaked, then used to inoculate liquid overnight cultures for storage
455 at -80˚C. Isolates were tested for the absence of cytochrome *C* oxidase using
456 Bactident Oxidase strips (Merck KgaA, Germany), characteristic of *P. syringae*. A total
457 of 148 *P. syringae* isolates were obtained from the four orchards (Table S1).

458 **PCR amplification & sequencing**

459 A lysate was prepared for each isolate by resuspending a colony in 100 µL ddH_20 and
460 lysing the cells at 96°C for 10 min. Strains were sequenced using the Hwang *et al*.
461 (2005) MLST scheme for four housekeeping genes *gapA*, *gyrB*, *gltA (=cts)* and *rpoD*
462 (reverse). Due to amplification problems, the forward primer for *rpoD* from Sarkar
463 and Guttman (2004) was used. PCR amplification was performed with a BIO-RAD

bioRxiv preprint doi: https://doi.org/10.1101/235853; this version posted December 18, 2017. The copyright holder for this preprint (which was not certified by peer review) is the author/funder. All rights reserved. No reuse allowed without permission.

464 T100 Thermal Cycler following an adapted protocol of Hwang et al. (2005): a total
465 reaction volume of 50 µl with a final concentration of 1x PCR buffer (Invitrogen, US),
466 1 µM for each primer, 0.2 mM dNTP's (Bioline, UK), 1 U Taq Polymerase (Invitrogen,
467 US), 1 µl lysed bacterial cells, 2% DMSO (Sigma-Aldrich, US) and 1.5 mM $MgCl_2$. Initial
468 denaturation was at 94°C for 2 min, followed by 30 cycles of amplification with
469 denaturation at 94°C for 30 s, annealing at 63°C for 30 s and elongation at 72°C for
470 1 min. Final elongation was for 3 min at 72°C. Samples were purified using the Exo-
471 CIP method and sequenced by Macrogen Inc (South Korea). Sequence analysis was
472 performed with Geneious v7.1.7 (Kearse *et al.*, 2012). Sequences were trimmed to
473 the same length (476 bp *gap1*, 507 bp *gyrB*, 529 bp *gltA*, 498 bp *rpoD*) and
474 concatenated (2010 bp) (GenBank accession numbers: *gapA* MG642149 -
475 MG642296; *gyrB* MG642297 - MG642444; *gltA* MG642445 - MG642592; *rpoD*
476 MG642593 - MG642740).

477 **Population genetics**

478 *Sequence diversity indices*

479 A rarefaction analysis was performed using MOTHUR v.1.34.4 by subsampling
480 using 1,000 iterations (Schloss *et al.*, 2009). Pairwise genetic distances between
481 isolates were calculated and sequences assigned to Operational Taxonomic Units
482 (OTUs) based on the corresponding average pairwise genetic distance of each group.

483 Simpson's index of diversity (D) and evenness (ED) (α-diversity) and
484 Sørensen's index of dissimilarity (β-diversity) were calculated using the *vegan*
485 package (Oksanen *et al.*, 2016) in R v3.3.1 (R.Core.Team, 2016). Simpson's D was

bioRxiv preprint doi: https://doi.org/10.1101/235853; this version posted December 18, 2017. The copyright holder for this preprint (which was not certified by peer review) is the author/funder. All rights reserved. No reuse allowed without permission.

486 converted to the effective number of species (D_c) in order to account for the non-
487 linear properties of Simpson's index of diversity (Jost, 2006).

488 *Multilocus Sequence Typing*

489 Sequence types (STs) sharing three out of four alleles (SLV, single locus
490 variants) were grouped using eBURST v3 (bootstrapped with 1,000,000 resamplings)
491 (Feil *et al.*, 2004; Spratt *et al.*, 2004). A Minimum Spanning Tree providing an
492 overview of triple locus variants was constructed using Phyloviz v2.0 (Francisco *et al.*,
493 2012).

494 165 non-redundant ST profiles of *P. syringae* strains were downloaded from
495 the Plant Associated and Environmental Microbes Database (PAMDB,
496 http://genome.ppws.vt.edu/cgi-bin/MLST/home.pl) (Almeida *et al.*, 2010). *P.*
497 *syringae* sequences isolated recently from kiwifruit and air in Japan (Tomihama *et*
498 *al.*, 2016) and kiwifruit isolates from NZ, France and the United States (Visnovsky *et*
499 *al.*, 2016) were also included. A reduced set of 37 *P. syringae* isolates representing
500 the different monophyletic groups of *P. syringae*, as well as the Japanese kiwifruit
501 strains and the US, France and NZ kiwifruit isolates from previous years were used to
502 provide better resolution in the phylogenies displayed in Figure 2 and Figure S4.

503 *Sequence diversity and recombination*

504 START2 (v0.9.0 beta) was employed to calculate parameters of genetic
505 diversity, number of alleles and polymorphic sites, GC content and the ratio of non-
506 synonymous to synonymous substitutions (d_N/d_S ratio) (Jolley *et al.*, 2001). The
507 number of mutations and amino acid changes and nucleotide diversity parameter π

bioRxiv preprint doi: https://doi.org/10.1101/235853; this version posted December 18, 2017. The copyright holder for this preprint (which was not certified by peer review) is the author/funder. All rights reserved. No reuse allowed without permission.

508 were calculated with DnaSP v. 5.10.1 (Rozas and Rozas, 1995). Jmodeltest 2.1.7
509 (Guindon and Gascuel, 2003; Darriba *et al.*, 2012) was used with default parameter
510 settings to find the best-fitting evolutionary model. Pairwise genetic variability
511 among and between phylogroups was calculated using MEGA7 (Kumar *et al.*, 2016).

512 To test whether genetic diversity varied by sampling location, time of
513 sampling, orchard infection status and/or cultivar, a permutational multivariate
514 analysis of variance (PERMANOVA) (Anderson, 2001; McArdle and Anderson, 2001)
515 was performed using PRIMER v 6.1.12 (PRIMER-E Ltd., Plymouth, UK, PERMANOVA+
516 add-on v. 1.0.2.). Pairwise distances among unique STs were used as input and tests
517 were run with 9999 permutations.

518 LDHAT v2.2a (Auton and McVean, 2007) was used to estimate the rate of
519 mutation (Watterson's θ) and recombination (ρ) using the composite likelihood
520 method of Hudson (Hudson, 2001) with an adaption to finite-site models. Only
521 polymorphic sites with two alleles were included and the frequency cut-off for
522 missing data was set to 0.2.

523 *Phylogenetic reconstruction*

524 Trees were built using single representatives of each unique ST from this
525 study to improve readability of the tree. TREEPUZZLE v5.3 (Schmidt *et al.*, 2002) was
526 used to construct maximum likelihood (ML) trees using the best-fitting evolutionary
527 model (jModeltest) for individual genes and the concatenated alignment (100,000
528 puzzling steps). Dnaml (PHYLIP v3.695, Felsenstein 1989) was used to test for

bioRxiv preprint doi: https://doi.org/10.1101/235853; this version posted December 18, 2017. The copyright holder for this preprint (which was not certified by peer review) is the author/funder. All rights reserved. No reuse allowed without permission.

529 congruence between single trees (SH-test) using default parameters, providing ML
530 trees as input and a random number seed of 333.

531 **Strains and culture conditions**

532 A list of all bacterial strains used in this study can be found in Table S2.
533 *Pseudomonas* strains were cultured in King's B or minimal M9 media at 28˚C and *E.*
534 *coli* was cultured in Luria Bertani medium at 37˚C. Liquid overnight cultures were
535 inoculated from single colonies and shaken at 250 rpm for 16 hrs. The antibiotics
536 kanamycin (kan) and nitrofurantoin (nf) were used at a concentration of 50 µg/ml.
537 Kanamycin resistant *Psa* NZ54 and *Psa* NZ13 Δ*hrcC* were employed in all *in vitro* and
538 *in planta* experiments.

539 **Mutant development**

540 *Psa* NZ13Δ*hrcC* was constructed by in-frame deletion of *hrcC* via marker
541 exchange mutagenesis. Knockout construct was generated by overlap extension PCR
542 (Ho *et al.*, 1989) using the primers listed in Table S6. DNA was amplified from *Psa*
543 NZ13 with Phusion® High-Fidelity DNA polymerase. The deletion construct was
544 inserted into pK18mobsacB (Schäfer *et al.*, 1994). The recombinant vector was
545 transferred into *Psa* NZ13 via triparental mating, using as helper *E. coli* DH5α strain
546 containing pRK2013. Mutants were selected by plating on KB kanamycin (50 µg/mL)
547 and subsequently on KB containing 5% sucrose. Mutants were screened by PCR using
548 external primers (Table S6) and the deletion was then confirmed by sequencing.

549 Triparental matings were performed to introduce a kanamycin resistant Tn*5*
550 transposon into *Psa* NZ54 and *Psa* NZ13 Δ*hrcC*. *E. coli* S17-1 Tn*5hah Sgid1* (donor)

bioRxiv preprint doi: https://doi.org/10.1101/235853; this version posted December 18, 2017. The copyright holder for this preprint (which was not certified by peer review) is the author/funder. All rights reserved. No reuse allowed without permission.

551 (Zhang *et al.*, 2015), *E. coli pRK2013* (helper) (Ditta *et al.*, 1980) and *Psa* NZ54 or *Psa*
552 NZ13 Δ*hrcC* (recipient) were grown in shaken liquid media overnight. 200 μl of donor
553 and helper and 2mL of recipient were individually washed, pelleted and combined in
554 30 μl 10 mM $MgCl_2$. The mixture was plated on a pre-warmed LB agar plate and
555 incubated at 28˚C for 24 hrs. The cells were scraped off and resuspended in 1 mL 10
556 mM $MgCl_2$ and plated on KB plates supplemented with kanamycin and
557 nitrofurantoin. Bacterial growth was compared to the wild type recipient in both KB
558 and M9 media to ensure marker introduction did not result in a loss of fitness.

559 **Competition assays**

560 *In vitro competition assays*

561 Competition experiments were performed *in vitro* using rich (King's B) and
562 minimal (M9) media in a shaken and static environment. Competition experiments
563 were performed in 1:1, 1:10 and 10:1 ratios for each of the four assay conditions.
564 Liquid overnight cultures of each strain in KB were established from single colony
565 inoculations. 30 mL vials with 4 mL of the appropriate media were inoculated with
566 each strain, adjusted to a founding density of either $5x10^6$ cfu ml^{-1} (OD_{600} 0.006) or
567 $4x10^4$ cfu ml^{-1} (OD_{600} 0.0004). Control vials were inoculated with a single strain,
568 adjusted to $5x10^6$ cfu ml^{-1}. Cultures were incubated at 28˚C and grown over a period
569 of 72 hrs, either still or shaken at 250rpm. Bacterial density was calculated at 0, 24,
570 48 and 72 hrs by plating dilutions on KB kan and M9 agar plates to distinguish
571 between competing strains. The experiment was performed using three replicates
572 and repeated three times.

bioRxiv preprint doi: https://doi.org/10.1101/235853; this version posted December 18, 2017. The copyright holder for this preprint (which was not certified by peer review) is the author/funder. All rights reserved. No reuse allowed without permission.

573 *In planta competition and pathogenicity assays*

574 Epiphytic and endophytic growth of *Psa* NZ54, *Psa* NZ13 Δ*hrcC* and *P.*
575 *syringae* G33C was evaluated on 4-week old kiwifruit plantlets using single and
576 mixed-culture inoculation. Clonally propagated *A. chinensis* var. *chinensis* 'Hort16A'
577 and 'SunGold' were grown for a minimum of one month in a Conviron CMP6010
578 growth cabinet at 21˚C with a 14/10 hr light/dark cycle and 70% humidity. Bacterial
579 strains were incubated for two days at 28˚C on KB plates, after which they were
580 resuspended in 10 mM $MgSO_4$ buffer. Mixed inoculum (1:1, 1:100 and 100:1) was
581 prepared in 50 mL 10 mM $MgSO_4$ buffer and 0.002% Silwet-70 (surfactant), with
582 strains adjusted to $8x10^7$ cfu ml^{-1} (OD_{600} 0.1) or $8x10^5$ cfu ml^{-1} (OD_{600} 0.001). Single
583 strain plant inoculations were also performed using an initial $8x10^7$ cfu ml^{-1} (OD_{600}
584 0.1).

585 Plants were inoculated by submerging leaves in the inoculum for 5 s and
586 allowing to air-dry. Plants were returned to the growth cabinet and watered every
587 second day. Bacterial density was assessed at either 0, 2, 4, 7 and 10 days post
588 inoculation (dpi) or 0, 3, and 7 dpi (Δ*hrcC* competition experiments). Epiphytic
589 growth was assessed by placing inoculated leaves in separate sterile plastic bags
590 with 35 mL 10 mM $MgSO_4$ buffer and shaking manually for 3 minutes. The leaf wash
591 was centrifuged at 4600 rpm for 3 min and the supernatant discarded. Bacteria were
592 resuspended in 200 µl buffer and serial dilutions plated on M9 and KB+kan agar
593 plates.

594 Endophytic growth was assessed by removing one $1cm^2$ leaf disk per plant
595 (including the midrib), surface sterilizing in 70% EtOH for 30 sec, drying and

bioRxiv preprint doi: https://doi.org/10.1101/235853; this version posted December 18, 2017. The copyright holder for this preprint (which was not certified by peer review) is the author/funder. All rights reserved. No reuse allowed without permission.

596 homogenising for 1 minute in a 1.5 mL Eppendorf tube containing 200 µl buffer and
597 two metal beads with the TissueLyser II (QIAGEN). The plant homogenate was
598 serially diluted and plated on M9 and KB+kan agar plates. All experiments were
599 performed in duplicate, with at least 4 replicates per experiment.

600 **Statistical analysis**

601 A Student's *t*-test was used to verify the statistical difference where
602 applicable. For non-normally distributed data with unequal variance, the Mann
603 Whitney U test was performed.

604 The fitness of each strain in the competition experiments is expressed as the
605 Malthusian parameter (Lenski *et al.*, 1991). The Malthusian parameter was
606 calculated as $M = (ln(N1_{f1}/N1_i))/(ln(N2_f/N2_i))$, where $N1_i$ is initial number of
607 cfu of strain 1 at 0h and $N1_f$ cfu after 24 hrs (*in vitro*) or 2/3 dpi (*in planta,*
608 'Hort16A'/'SunGold').

609 **BIOSECURITY AND APPROVAL**

610 All worked was performed in approved facilities and in accord with APP201675,
611 APP201730, APP202231.

612 **ACKNOWLEDGEMENTS**

613 We want to particularly thank kiwifruit growers David French, Rex Reed and Bruce
614 and Fiona Aitken for granting access to their orchards. The work conducted was
615 supported the New Zealand Ministry for Business, Innovation and Employment

bioRxiv preprint doi: https://doi.org/10.1101/235853; this version posted December 18, 2017. The copyright holder for this preprint (which was not certified by peer review) is the author/funder. All rights reserved. No reuse allowed without permission.

616 (C11X1205). Christina Straub was supported through a PhD scholarship from the
617 New Zealand Institute for Advanced Studies (NZIAS) and Plant & Food Research.

618 **REFERENCES**

619 Abelleira, A., López, M.M., Peñalver, J., Aguín, O., Mansilla, J.P., Picoaga, A., and
620 García, M.J. (2011) First report of bacterial canker of kiwifruit Caused by
621 Pseudomonas syringae pv. actinidiae in Spain. *Plant Dis.* **95**: 1583.
622 Adams, P.D. and Kloepper, J.W. (2002) Effect of host genotype on indigenous
623 bacterial endophytes of cotton (Gossypium hirsutum L.). *Plant Soil* **240**: 181–
624 189.
625 Almeida, N.F., Yan, S., Cai, R., Clarke, C.R., Morris, C.E., Schaad, N.W., et al. (2010)
626 PAMDB, a multilocus sequence typing and analysis database and website for
627 plant-associated microbes. *Phytopathology* **100**: 208–215.
628 Anderson, M.J. (2001) A new method for non parametric multivariate analysis of
629 variance. *Austral Ecol.* **26**: 32–46.
630 Auton, A. and McVean, G. (2007) Recombination rate estimation in the presence of
631 hotspots. *Genome Res.* **17**: 1219–1227.
632 Balestra, G.M., Mazzaglia, A., Spinelli, R., Graziani, S., Quattrucci, A., and Rossetti, A.
633 (2008) Cancro batterico su Actinidia chinensis. *L'informatore Agrar.* **38**: 75–76.
634 Baltrus, D.A., Nishimura, M.T., Romanchuk, A., Chang, J.H., Mukhtar, M.S., Cherkis,
635 K., et al. (2011) Dynamic evolution of pathogenicity revealed by sequencing and
636 comparative genomics of 19 Pseudomonas syringae isolates. *PLoS Pathog.* **7**:
637 e1002132.
638 Bartoli, C., Berge, O., Monteil, C.L., Guilbaud, C., Balestra, G.M., Varvaro, L., et al.
639 (2014) The Pseudomonas viridiflava phylogroups in the P. syringae species
640 complex are characterized by genetic variability and phenotypic plasticity of
641 pathogenicity-related traits. *Environ. Microbiol.* **16**: 2301–2315.
642 Bartoli, C., Lamichhane, J.R., Berge, O., Guilbaud, C., Varvaro, L., Balestra, G.M., et al.
643 (2015) A framework to gauge the epidemic potential of plant pathogens in
644 environmental reservoirs: the example of kiwifruit canker. *Mol. Plant Pathol.*
645 **16**: 137–49.
646 Beiki, F., Busquets, A., Gomila, M., Rahimian, H., Lalucat, J., and García-Valdés, E.
647 (2016) New Pseudomonas spp. are pathogenic to citrus. *PLoS One* **11**:
648 e0148796.
649 Bender, C.L., Alarcon-Chaidez, F., Gross, D.C., Alarcón-Chaidez, F., and Gross, D.C.
650 (1999) Pseudomonas syringae phytotoxins: Mode of action, regulation, and
651 biosynthesis by peptide and polyketide synthetases. *Microbiol. Mol. Biol. Rev.*
652 **63**: 266–292.
653 Berge, O., Monteil, C.L., Bartoli, C., Chandeysson, C., Guilbaud, C., Sands, D.C., and
654 Morris, C.E. (2014) A user's guide to a data base of the diversity of
655 Pseudomonas syringae and its application to classifying strains in this
656 phylogenetic complex. *PLoS One* **9**: e105547.
657 Berlec, A. (2012) Novel techniques and findings in the study of plant microbiota:

bioRxiv preprint doi: https://doi.org/10.1101/235853; this version posted December 18, 2017. The copyright holder for this preprint (which was not certified by peer review) is the author/funder. All rights reserved. No reuse allowed without permission.

658 Search for plant probiotics. *Plant Sci.* **193–194**: 96–102.
659 Bodenhausen, N., Bortfeld-Miller, M., Ackermann, M., and Vorholt, J.A. (2014) A
660 Synthetic Community Approach Reveals Plant Genotypes Affecting the
661 Phyllosphere Microbiota. *PLoS Genet.* **10**: e1004283.
662 Bratcher, H.B., Corton, C., Jolley, K.A., Parkhill, J., and Maiden, M.C. (2014) A gene-
663 by-gene population genomics platform: de novo assembly, annotation and
664 genealogical analysis of 108 representative Neisseria meningitidis genomes.
665 *BMC Genomics* **15**: 1138.
666 Bull, C.T., Clarke, C.R., Cai, R., Vinatzer, B.A., Jardini, T.M., and Koike, S.T. (2011)
667 Multilocus sequence typing of Pseudomonas syringae sensu lato confirms
668 previously described genomospecies and permits rapid identification of P.
669 syringae pv. coriandricola and P. syringae pv. apii causing bacterial leaf spot on
670 parsley. *Phytopathology* **101**: 847–858.
671 Buonaurio, R., Moretti, C., da Silva, D.P., Cortese, C., Ramos, C., and Venturi, V.
672 (2015) The olive knot disease as a model to study the role of interspecies
673 bacterial communities in plant disease. *Front. Plant Sci.* **6**: 1–12.
674 Cameron, A. and Sarojini, V. (2014) Pseudomonas syringae pv. actinidiae: chemical
675 control, resistance mechanisms and possible alternatives. *Plant Pathol.* **63**:.
676 Caugant, D.A. and Maiden, M.C.J. (2009) Meningococcal carriage and disease—
677 Population biology and evolution. *Vaccine* **27**: B64–B70.
678 Colombi, E., Straub, C., Künzel, S., Templeton, M.D., McCann, H.C., and Rainey, P.B.
679 (2017) Evolution of copper resistance in the kiwifruit pathogen Pseudomonas
680 syringae pv. actinidiae through acquisition of integrative conjugative elements
681 and plasmids. *Environ. Microbiol.* **19**: 819–832.
682 Cordero, O.X., Wildschutte, H., Kirkup, B., Proehl, S., Ngo, L., Hussain, F., et al. (2012)
683 Ecological Populations of Bacteria Act as Socially Cohesive Units of Antibiotic
684 Production and Resistance. *Science (80-.).* **337**: 1228–1231.
685 Darriba, D., Taboada, G.L., Doallo, R., and Posada, D. (2012) jModelTest 2: more
686 models, new heuristics and parallel computing. *Nat. Methods* **9**: 772–772.
687 Demba Diallo, M., Monteil, C.L., Vinatzer, B.A., Clarke, C.R., Glaux, C., Guilbaud, C., et
688 al. (2012) Pseudomonas syringae naturally lacking the canonical type III
689 secretion system are ubiquitous in nonagricultural habitats, are phylogenetically
690 diverse and can be pathogenic. *ISME J.* **6**: 1325–1335.
691 Ditta, G., Stanfield, S., Corbin, D., and Helinski, D.R. (1980) Broad host range DNA
692 cloning system for gram-negative bacteria: construction of a gene bank of
693 Rhizobium meliloti. *Proc. Natl. Acad. Sci.* **77**: 7347–7351.
694 Essakhi, S., Cesbron, S., Fischer-Le Saux, M., Bonneau, S., Jacques, M.A., and
695 Manceau, C. (2015) Phylogenetic and variable-number tandem-repeat analyses
696 identify nonpathogenic Xanthomonas arboricola lineages lacking the canonical
697 type III secretion system. *Appl. Environ. Microbiol.* **81**: 5395–5410.
698 Everett, K.R., Taylor, R.K., Romberg, M.K., Rees-George, J., Fullerton, R.A., Vanneste,
699 J.L., and Manning, M.A. (2011) First report of Pseudomonas syringae pv.
700 actinidiae causing kiwifruit bacterial canker in New Zealand. *Australas. Plant*
701 *Dis. Notes* **6**: 67–71.
702 Feil, E.J., Li, B.C., Aanensen, D.M., Hanage, W.P., and Spratt, B.G. (2004) eBURST:
703 inferring patterns of evolutionary descent among clusters of related bacterial
704 genotypes from Multilocus Sequence Typing Data. *J. Bacteriol.* **186**: 1518–1530.

bioRxiv preprint doi: https://doi.org/10.1101/235853; this version posted December 18, 2017. The copyright holder for this preprint (which was not certified by peer review) is the author/funder. All rights reserved. No reuse allowed without permission.

705 Felsenstein, J. (1989) Phylip: phylogeny inference package (version 3.2). *Cladistics* **5**:
706 164–166.
707 Ferrante, P. and Scortichini, M. (2010) Molecular and phenotypic features of
708 Pseudomonas syringae pv. actinidiae isolated during recent epidemics of
709 bacterial canker on yellow kiwifruit (Actinidia chinensis) in central Italy. *Plant*
710 *Pathol.* **59**: 954–962.
711 Francisco, A.P., Vaz, C., Monteiro, P.T., Melo-Cristino, J., Ramirez, M., and Carriço,
712 J.A. (2012) PHYLOViZ: phylogenetic inference and data visualization for
713 sequence based typing methods. *BMC Bioinformatics* **13**: 87.
714 Fraser, C., Hanage, W.P., and Spratt, B.G. (2005) Neutral microepidemic evolution of
715 bacterial pathogens. *Proc. Natl. Acad. Sci.* **102**: 1968–1973.
716 Fujikawa, T. and Sawada, H. (2016) Genome analysis of the kiwifruit canker pathogen
717 Pseudomonas syringae pv. actinidiae biovar 5. *Sci. Rep.* **6**:.
718 Fukami, T., Beaumont, H.J.E., Zhang, X.-X., and Rainey, P.B. (2007) Immigration
719 history controls diversification in experimental adaptive radiation. *Nature* **446**:
720 436–439.
721 Goss, E.M., Kreitman, M., and Bergelson, J. (2005) Genetic diversity, recombination
722 and cryptic clades in Pseudomonas viridiflava infecting natural populations of
723 Arabidopsis thaliana. *Genetics* **169**: 21–35.
724 Guindon, S. and Gascuel, O. (2003) A simple, fast, and accurate algorithm to estimate
725 large phylogenies by maximum likelihood. *Syst. Biol.* **52**: 696–704.
726 Haapalainen, M., Mosorin, H., Dorati, F., Wu, R.F., Roine, E., Taira, S., et al. (2012)
727 Hcp2, a secreted protein of the phytopathogen Pseudomonas syringae pv.
728 tomato DC3000, is required for fitness for competition against bacteria and
729 yeasts. *J. Bacteriol.* **194**: 4810–4822.
730 Hall, S.J., Dry, I.B., Blanchard, C.L., and Whitelaw-Weckert, M.A. (2016) Phylogenetic
731 relationships of Pseudomonas syringae pv. syringae isolates associated with
732 bacterial iInflorescence rot in grapevine. *Plant Dis.* **100**: 607–616.
733 Han, H.S., Nam, H.Y., Koh, Y.J., Hur, J.-S., and Jung, J.S. (2003) Molecular bases of
734 high-level streptomycin resistance in Pseudomonas marginalis and
735 Pseudomonas syringae pv. actinidiae. *J. Microbiol.* **41**: 16–21.
736 Haubold, B. and Rainey, P.B. (1996) Genetic and ecotypic structure of a fluorescent
737 Pseudomonas population. *Mol. Ecol.* **5**: 747–761.
738 Hayes, C.S., Aoki, S.K., and Low, D.A. (2010) Bacterial contact-dependent delivery
739 systems. *Annu. Rev. Genet.* **44**: 71–90.
740 Hernández-Morales, A., De la Torre-Zavala, S., Ibarra-Laclette, E., Hernández-Flores,
741 J., Jofre-Garfias, A., Martínez-Antonio, A., and Álvarez-Morales, A. (2009)
742 Transcriptional profile of Pseudomonas syringae pv. phaseolicola NPS3121 in
743 response to tissue extracts from a susceptible Phaseolus vulgaris L. cultivar.
744 *BMC Microbiol.* **9**: 257.
745 Hibbing, M.E., Fuqua, C., Parsek, M.R., and Peterson, S.B. (2010) Bacterial
746 competition: surviving and thriving in the microbial jungle. *Nat. Rev. Microbiol.*
747 **8**: 15–25.
748 Hirano, S.S., Charkowski, A.O., Collmer, A., Willis, D.K., and Upper, C.D. (1999) Role of
749 the Hrp type III protein secretion system in growth of Pseudomonas syringae
750 pv. syringae B728a on host plants in the field. *Proc. Natl. Acad. Sci.* **96**: 9851–
751 9856.

bioRxiv preprint doi: https://doi.org/10.1101/235853; this version posted December 18, 2017. The copyright holder for this preprint (which was not certified by peer review) is the author/funder. All rights reserved. No reuse allowed without permission.

752 Hirano, S.S. and Upper, C.D. (2000) Bacteria in the leaf ecosystem with emphasis on
753 Pseudomonas syringae - a pathogen, ice nucleus, and epiphyte. *Microbiol. Mol.*
754 *Biol. Rev.* **64**: 624–653.
755 Ho, S.N., Hunt, H.D., Horton, R.M., Pullen, J.K., and Pease, L.R. (1989) Site-directed
756 mutagenesis by overlap extension using the polymerase chain reaction. *Gene*
757 **77**: 51–59.
758 Hockett, K.L., Renner, T., and Baltrus, D.A. (2015) Independent co-option of a tailed
759 bacteriophage into a killing complex in Pseudomonas. *MBio* **6**: 1–11.
760 Hudson, R.R. (2001) Two-locus sampling distributions and their application. *Genetics*
761 **159**: 1805–1817.
762 Humphrey, P.T., Nguyen, T.T., Villalobos, M.M., and Whiteman, N.K. (2014) Diversity
763 and abundance of phyllosphere bacteria are linked to insect herbivory. *Mol.*
764 *Ecol.* **23**: 1497–1515.
765 Hwang, M.S.H., Morgan, R.L., Sarkar, S.F., Wang, P.W., and Guttman, D.S. (2005)
766 Phylogenetic characterization of virulence and resistance phenotypes of
767 Pseudomonas syringae. *Appl. Environ. Microbiol.* **71**: 5182–5191.
768 Istock, C.A., Duncan, K.E., Ferguson, N., and Zhou, X. (1992) Sexuality in a natural
769 population of bacteria - Bacillus subtilis challenges the clonal paradigm. *Mol.*
770 *Ecol.* **1**: 95–103.
771 Jolley, K.A., Feil, E.J., Chan, M.S., and Maiden, M.C. (2001) Sequence type analysis
772 and recombinational tests (START). *Bioinformatics* **17**: 1230–1231.
773 Jost, L. (2006) Entropy and diversity. *Oikos* **113**: 363–375.
774 Karasov, T.L., Barrett, L., Hershberg, R., and Bergelson, J. (2017) Similar levels of gene
775 content variation observed for Pseudomonas syringae populations extracted
776 from single and multiple host species. *PLoS One* **12**: 1–18.
777 Kearse, M., Moir, R., Wilson, A., Stones-Havas, S., Cheung, M., Sturrock, S., et al.
778 (2012) Geneious Basic: An integrated and extendable desktop software
779 platform for the organization and analysis of sequence data. *Bioinformatics* **28**:
780 1647–1649.
781 Kniskern, J.M., Barrett, L.G., and Bergelson, J. (2011) Maladaptation in wild
782 populations of the generalist plant pathogen Pseudomonas syringae. *Evolution*
783 *(N. Y).* **65**: 818–830.
784 Koh, Y.J., Kim, G.H., Koh, H.S., Lee, Y.S., Kim, S.C., and Jung, J.S. (2012) Occurrence of
785 a new type of Pseudomonas syringae pv. actinidiae strain of bacterial canker on
786 kiwifruit in Korea. *Plant Pathol.* **28**: 423–427.
787 Kõiv, V., Roosaare, M., Vedler, E., Ann Kivistik, P., Toppi, K., Schryer, D.W., et al.
788 (2015) Microbial population dynamics in response to Pectobacterium
789 atrosepticum infection in potato tubers. *Sci. Rep.* **5**: 11106.
790 Kumar, S., Stecher, G., and Tamura, K. (2016) MEGA7: Molecular Evolutionary
791 Genetics Analysis version 7.0 for bigger datasets. *Mol. Biol. Evol.* **33**: 1870–1874.
792 Laforest-Lapointe, I., Messier, C., Kembel, S.W., Lindow, S., Brandl, M., Herre, E., et
793 al. (2016) Host species identity, site and time drive temperate tree phyllosphere
794 bacterial community structure. *Microbiome* **4**: 27.
795 Lamichhane, J.R. and Venturi, V. (2015) Synergisms between microbial pathogens in
796 plant disease complexes: a growing trend. *Front. Plant Sci.* **6**: 385.
797 Lenski, R.E., Rose, M.R., Simpson, S.C., and Tadler, S.C. (1991) Long-term
798 experimental evolution in Escherichia coli . I . Adaptation and divergence during

bioRxiv preprint doi: https://doi.org/10.1101/235853; this version posted December 18, 2017. The copyright holder for this preprint (which was not certified by peer review) is the author/funder. All rights reserved. No reuse allowed without permission.

799 2,000 generations. *Am. Nat.* **138**: 1315–1341.
800 Lindow, S.E. (1986) Construction of isogenic Ice strains of Pseudomonas syringae for
801 evaluation of specificity of competition on leaf surfaces. *Perspect. Microb. Ecol.*
802 *Slov. Soc. Microbiol. Ljubljana* 509–515.
803 Lindow, S.E. and Brandl, M.T. (2003) Microbiology of the phyllosphere. *Appl. Environ.*
804 *Microbiol.* **69**: 1875–1883.
805 Macho, A.P., Zumaquero, A., Ortiz-Martín, I., and Beuzón, C.R. (2007) Competitive
806 index in mixed infections: A sensitive and accurate assay for the genetic analysis
807 of Pseudomonas syringae-plant interactions. *Mol. Plant Pathol.* **8**: 437–450.
808 Marchi, G., Sisto, A., Cimmino, A., Andolfi, A., Cipriani, M.G., Evidente, A., and Surico,
809 G. (2006) Interaction between Pseudomonas savastanoi pv. savastanoi and
810 Pantoea agglomerans in olive knots. *Plant Pathol.* **55**: 614–624.
811 Maynard Smith, J., Smith, N.H., O'Rourke, M., and Spratt, B.G. (1993) How clonal are
812 bacteria? *Proc. Natl. Acad. Sci.* **90**: 4384–4388.
813 McArdle, B.H. and Anderson, M.J. (2001) Fitting multivariate models to community
814 data: a comment on distance-based redundancy analysis. *Ecology* **82**: 290–297.
815 McCann, H.C., Li, L.L., Liu, Y., Li, D., Pan, H., Zhong, C., et al. (2017) Origin and
816 evolution of the kiwifruit canker pandemic. *Genome Biol. Evol.* **9**: 932–944.
817 McCann, H.C., Rikkerink, E.H.A., Bertels, F., Fiers, M., Lu, A., Rees-George, J., et al.
818 (2013) Genomic analysis of the kiwifruit pathogen Pseudomonas syringae pv.
819 actinidiae provides insight into the origins of an emergent plant disease. *PLoS*
820 *Pathog.* **9**: e1003503.
821 Mohr, T.J., Liu, H., Yan, S., Morris, C.E., Castillo, J.A., Jelenska, J., and Vinatzer, B.A.
822 (2008) Naturally occurring nonpathogenic isolates of the plant pathogen
823 Pseudomonas syringae lack a type III secretion system and effector gene
824 orthologues. *J. Bacteriol.* **190**: 2858–2870.
825 Monier, J.-M. and Lindow, S.E. (2003) Differential survival of solitary and aggregated
826 bacterial cells promotes aggregate formation on leaf surfaces. *Proc. Natl. Acad.*
827 *Sci.* **100**: 15977–15982.
828 Moretti, C., Hosni, T., Vandemeulebroecke, K., Brady, C., de Vos, P., Buonaurio, R.,
829 and Cleenwerck, I. (2011) Erwinia oleae sp. nov., isolated from olive knots
830 caused by Pseudomonas savastanoi pv. savastanoi. *Int. J. Syst. Evol. Microbiol.*
831 **61**: 2745–2752.
832 Morris, C.E., Sands, D.C., Vanneste, J.L., Montarry, J., Oakley, B., Guilbaud, C., and
833 Glaux, C. (2010) Inferring the evolutionary history of the plant pathogen
834 Pseudomonas syringae from its biogeography in headwaters of rivers in North
835 America, Europe, and New Zealand. *MBio* **1**: e00107.
836 Nakahara, H., Mori, T., Sadakari, N., Matsusaki, H., and Matsuzoe, N. (2016) Selection
837 of effective non-pathogenic Ralstonia solanacearum as biocontrol agents
838 against bacterial wilt in eggplant. *J. Plant Dis. Prot.* **123**: 119–124.
839 Nowell, R.W., Laue, B.E., Sharp, P.M., and Green, S. (2016) Comparative genomics
840 reveals genes significantly associated with woody hosts in the plant pathogen
841 Pseudomonas syringae. *Mol. Plant Pathol.* **17**: 1409–1424.
842 Oksanen, J., Blanchet, F.G., Friendly, M., Kindt, R., Legendre, P., Dan McGlinn, Peter
843 R. Minchin, R.B.O., et al. (2016) vegan: Community Ecology Package.
844 Omer, M.E.H. and Wood, R.K.S. (1969) Growth of Pseudomonas phaseolicola in
845 susceptible and in resistant bean plants. *Ann. Appl. Biol.* **63**: 103–116.

bioRxiv preprint doi: https://doi.org/10.1101/235853; this version posted December 18, 2017. The copyright holder for this preprint (which was not certified by peer review) is the author/funder. All rights reserved. No reuse allowed without permission.

846 Van Overbeek, L. and Van Elsas, J.D. (2008) Effects of plant genotype and growth
847 stage on the structure of bacterial communities associated with potato
848 (Solanum tuberosum L.). *FEMS Microbiol. Ecol.* **64**: 283–296.
849 Petriccione, M., Zampella, L., Mastrobuoni, F., and Scortichini, M. (2017) Occurrence
850 of copper-resistant Pseudomonas syringae pv. syringae strains isolated from
851 rain and kiwifruit orchards also infected by P. s. pv. actinidiae. *Eur. J. Plant*
852 *Pathol.* 1–16.
853 Pfeilmeier, S., Caly, D.L., and Malone, J.G. (2016) Bacterial pathogenesis of plants:
854 future challenges from a microbial perspective: Challenges in Bacterial
855 Molecular Plant Pathology. *Mol. Plant Pathol.* **17**: 1298–1313.
856 Polz, M.F., Alm, E.J., and Hanage, W.P. (2013) Horizontal gene transfer and the
857 evolution of bacterial and archaeal population structure. *Trends Genet.* **29**:
858 170–175.
859 R.Core.Team (2016) R: A language and environment for statistical computing.
860 Rosen, M.J., Davison, M., Bhaya, D., and Fisher, D.S. (2015) Fine-scale diversity and
861 extensive recombination in a quasisexual bacterial population occupying a
862 broad niche. *Science (80-.).* **348**: 1019–1024.
863 Rozas, J. and Rozas, R. (1995) DnaSP, DNA sequence polymorphism: an interactive
864 program for estimating population genetics parameters from DNA sequence
865 data. *CABIOS* **11**: 621–625.
866 Rufián, J.S., Macho, A.P., Corry, D.S., Mansfield, J., Arnold, D., and Beuzón, C.R.
867 (2017) Confocal microscopy reveals in planta dynamic interactions between
868 pathogenic, avirulent and non-pathogenic Pseudomonas syringae strains. *Mol.*
869 *Plant Pathol.* DOI: 10.1111/mpp.12539.
870 Ruhe, Z.C., Low, D.A., and Hayes, C.S. (2013) Bacterial contact-dependent growth
871 inhibition. *Trends Microbiol.* **21**: 230–237.
872 Sarkar, S.F. and Guttman, D.S. (2004) Evolution of the core genome of Pseudomonas
873 syringae, a highly clonal, endemic plant pathogen. *Appl. Environ. Microbiol.* **70**:
874 1999–2012.
875 Sawada, H. (2015) Characterization of biovar 3 strains of Pseudomonas syringae pv.
876 actinidiae isolated in Japan. *Japanese J. Phyopathology* **81**: 111–126.
877 Sawada, H.H., Suzuki, F.F., Matsuda, I.I., and Saitou, N.N. (1999) Phylogenetic
878 analysis of Pseudomonas syringae pathovars suggests the horizontal gene
879 transfer of argK and the evolutionary stability of hrp gene cluster. *J. Mol. Evol.*
880 **49**: 627–644.
881 Schäfer, A., Tauch, A., Jäger, W., Kalinowski, J., Thierbach, G., and Pühler, A. (1994)
882 Small mobilizable multi-purpose cloning vectors derived from the Escherichia
883 coli plasmids pK18 and pK19: selection of defined deletions in the chromosome
884 of Corynebacterium glutamicum. *Gene* **145**: 69–73.
885 Schloss, P.D., Westcott, S.L., Ryabin, T., Hall, J.R., Hartmann, M., Hollister, E.B., et al.
886 (2009) Introducing mothur: Open-source, platform-independent, community-
887 supported software for describing and comparing microbial communities. *Appl.*
888 *Environ. Microbiol.* **75**: 7537–7541.
889 Schmidt, H.A., Strimmer, K., Vingron, M., and von Haeseler, A. (2002) TREE-PUZZLE:
890 maximum likelihood phylogenetic analysis using quartets and parallel
891 computing. *Bioinformatics* **18**: 502–504.
892 Shapiro, B.J., Friedman, J., Cordero, O.X., Preheim, S.P., Timberlake, S.C., Szabo, G.,

bioRxiv preprint doi: https://doi.org/10.1101/235853; this version posted December 18, 2017. The copyright holder for this preprint (which was not certified by peer review) is the author/funder. All rights reserved. No reuse allowed without permission.

893 et al. (2012) Population Genomics of Early Events in the Ecological
894 Differentiation of Bacteria. *Science (80-.).* **336**: 48–51.
895 Shapiro, B.J. and Polz, M.F. (2014) Ordering microbial diversity into ecologically and
896 genetically cohesive units. *Trends Microbiol.* **22**: 235–247.
897 Singer, M. (2010) Pathogen-pathogen interaction. *Virulence* **1**: 10–18.
898 Souza, V., Nguyen, T.T., Hudson, R.R., Piñero, D., and Lenski, R.E. (1992) Hierarchical
899 analysis of linkage disequilibrium in Rhizobium populations: evidence for sex?
900 *Proc. Natl. Acad. Sci. U. S. A.* **89**: 8389–93.
901 Spratt, B.G., Hanage, W.P., Li, B., Aanensen, D.M., and Feil, E.J. (2004) Displaying the
902 relatedness among isolates of bacterial species -- the eBURST approach. *FEMS*
903 *Microbiol. Lett.* **241**: 129–134.
904 Spratt, B.G. and Maiden, M.C.J. (1999) Bacterial population genetics, evolution and
905 epidemiology. *Philos. Trans. R. Soc. B Biol. Sci.* **354**: 701–710.
906 Stubbendieck, R.M., Vargas-Bautista, C., and Straight, P.D. (2016) Bacterial
907 communities: Interactions to scale. *Front. Microbiol.* **7**: 1234.
908 Tomihama, T., Sekita, T., and Takikawa, Y. (2016) Wide distribution of airborne ice-
909 nucleation active Pseudomonas syringae in agricultural environments.
910 *Phytopathology* **5159**: 1–49.
911 Triplett, L.R., Verdier, V., Campillo, T., Van Malderghem, C., Cleenwerck, I., Maes, M.,
912 et al. (2015) Characterization of a novel clade of Xanthomonas isolated from
913 rice leaves in Mali and proposal of Xanthomonas maliensis sp. nov. *Antonie van*
914 *Leeuwenhoek, Int. J. Gen. Mol. Microbiol.* **107**: 869–881.
915 Visnovsky, S.B., Fiers, M., Lu, A., Panda, P., Taylor, R., and Pitman, A.R. (2016) Draft
916 genome sequences of 18 strains of Pseudomonas isolated from kiwifruit plants
917 in New Zealand and overseas. *Genome Announc.* **4**: e00061-16.
918 Völksch, B. and May, R. (2001) Biological Control of Pseudomonas syringae pv.
919 glycinea by Epiphytic Bacteria under Field Conditions. *Microb. Ecol.* **41**: 132–
920 139.
921 Wagner, M.R., Lundberg, D.S., del Rio, T.G., Tringe, S.G., Dangl, J.L., and Mitchell-
922 Olds, T. (2016) Host genotype and age shape the leaf and root microbiomes of a
923 wild perennial plant. *Nat. Commun.* **7**: 12151.
924 Whipps, J.M., Hand, P., Pink, D., and Bending, G.D. (2008) Phyllosphere microbiology
925 with special reference to diversity and plant genotype. *J. Appl. Microbiol.* **105**:
926 1744–1755.
927 Wilson, M., Hirano, S.S., and Lindow, S.E. (1999) Location and survival of leaf-
928 associated bacteria in relation to pathogenicity and potential for growth within
929 the leaf. *Appl. Environ. Microbiol.* **65**: 1435–1443.
930 Wilson, M. and Lindow, S.E. (1994) Coexistence among epiphytic bacterial
931 Populations mediated through nutritional resource partitioning. *Appl. Environ.*
932 *Microbiol.* **60**: 4468–4477.
933 Young, J.M. (1974) Development of bacterial populations in vivo in relation to plant
934 pathogenicity. *New Zeal. J. Agric. Res.* **17**: 105–113.
935 Zhang, X.X., Gauntlett, J.C., Oldenburg, D.G., Cook, G.M., and Rainey, P.B. (2015) Role
936 of the transporter-like sensor kinase CbrA in histidine uptake and signal
937 transduction. *J. Bacteriol.* **197**: 2867–2878.
938 Zhao, Z.B., Gao, X.N., Huang, Q.L., Huang, L.L., Qin, H.Q., and Kang, Z.S. (2013)
939 Identification and characerization of the causal agent of bacterial canker of

bioRxiv preprint doi: https://doi.org/10.1101/235853; this version posted December 18, 2017. The copyright holder for this preprint (which was not certified by peer review) is the author/funder. All rights reserved. No reuse allowed without permission.

940 kiwifruit in the Shaanxi province of China. *J. Plant Pathol.* **95**: 155–162.

941

942 **FIGURES**

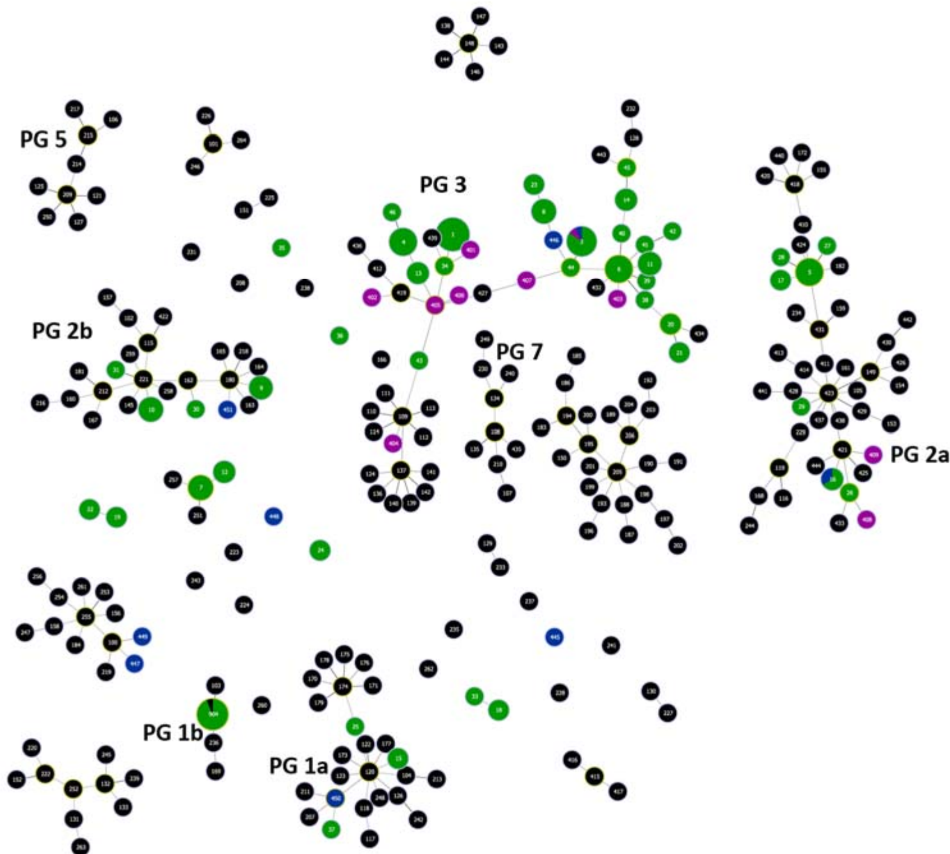

943

944

945 **Figure 1. Global Minimum Spanning Tree (MST).** Displaying the relationships
946 between STs at the triple-locus-variant level, illustrated using PHYLOViZ (Francisco *et*
947 *al.*, 2012). The size of the circle correlates with the frequency of the ST. Color-coded
948 accorded to origin: green = this study, black = PAMDB, blue = Visnovsky *et al.* (2016),
949 purple = Tomihama *et al.* (2016).

950

bioRxiv preprint doi: https://doi.org/10.1101/235853; this version posted December 18, 2017. The copyright holder for this preprint (which was not certified by peer review) is the author/funder. All rights reserved. No reuse allowed without permission.

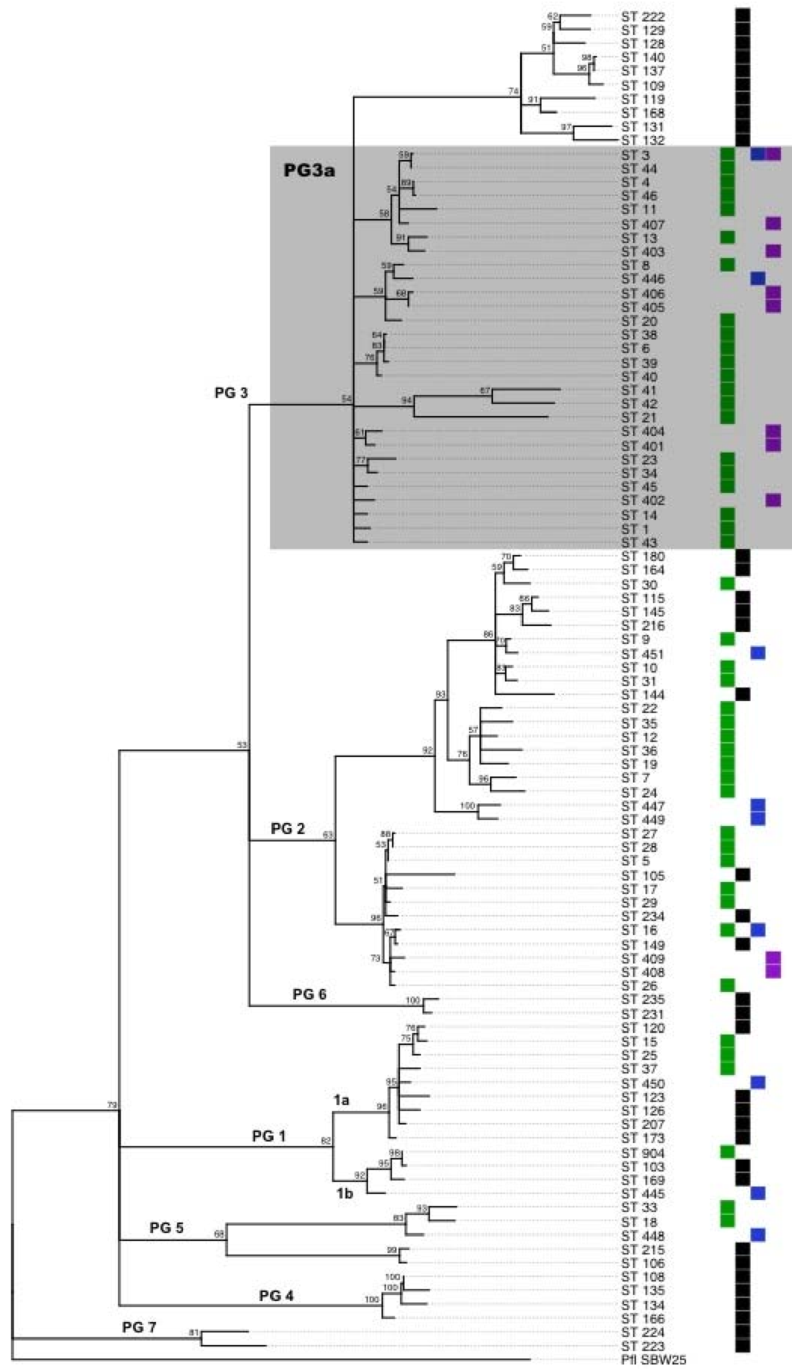

951

bioRxiv preprint doi: https://doi.org/10.1101/235853; this version posted December 18, 2017. The copyright holder for this preprint (which was not certified by peer review) is the author/funder. All rights reserved. No reuse allowed without permission.

952 **Figure 2. Maximum Likelihood tree based on the concatenated alignment (2010**
953 **bp) of four housekeeping genes: *gapA*, *gyrB*, *gltA* and *rpoD*.** Maximum Likelihood
954 tree reconstructed using TREEPUZZLE based on the Tamura-Nei model using 100,000
955 puzzling steps. Single representative sequences for each ST were used to improve
956 readability (frequency of each ST and corresponding strain names listed in Table S2).
957 Values indicated at nodes are bootstrap values. The corresponding phylogroups (PG)
958 are indicated, eg. PG1 = phylogroup 1 with clades 1a and 1b. Origin of isolates is
959 illustrated in colour coded boxes, green = this study, black = PAMDB, blue =
960 Visnovsky et al. 2016, purple = Tomihama et al. 2016

961

bioRxiv preprint doi: https://doi.org/10.1101/235853; this version posted December 18, 2017. The copyright holder for this preprint (which was not certified by peer review) is the author/funder. All rights reserved. No reuse allowed without permission.

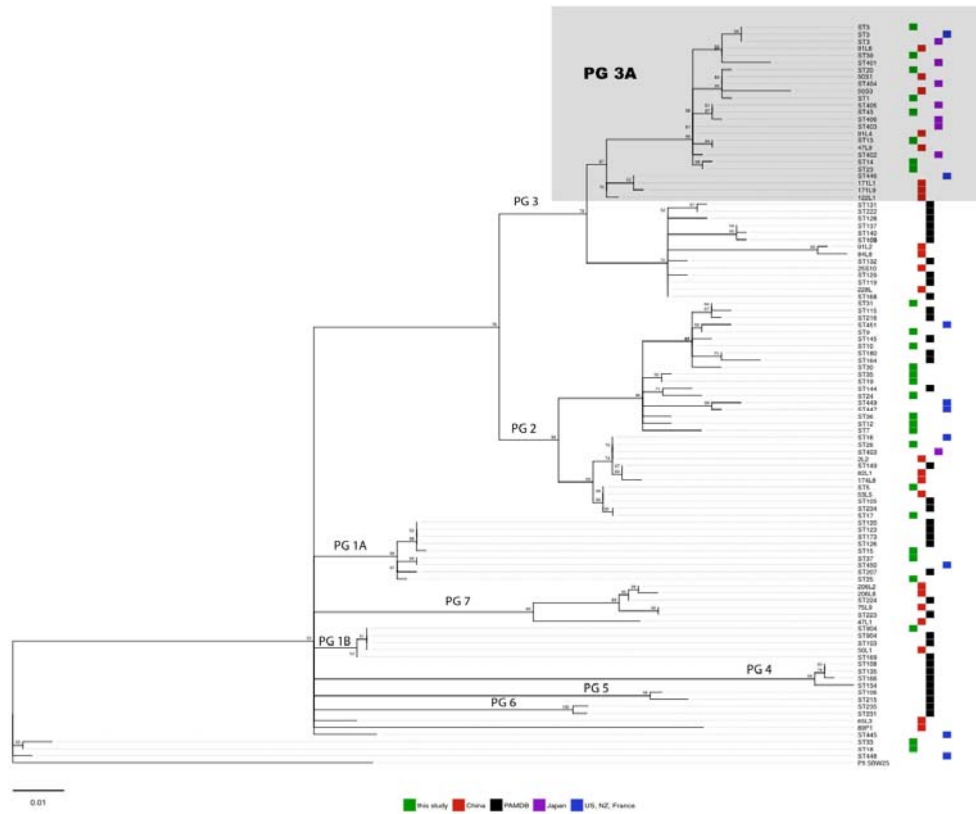

962

963 **Figure 3. Global ML tree reconstructed from *gltA* sequences highlighting the**
964 **particularity of PG3a, which includes kiwifruit isolates from NZ, China, Japan, the**
965 **US and France.** The tree was built on a 529 bp alignment using TREEPUZZLE (HKY
966 model; 100,000 puzzling steps), using *Pseudomonas fluorescens* SBW25 as outgroup.
967 Values indicated at nodes are bootstrap values. The source of each isolate is
968 highlighted in colour-coded boxes, green = this study, red = China, black = PAMDB,
969 purple = Japan, blue = US, NZ and France.

970

bioRxiv preprint doi: https://doi.org/10.1101/235853; this version posted December 18, 2017. The copyright holder for this preprint (which was not certified by peer review) is the author/funder. All rights reserved. No reuse allowed without permission.

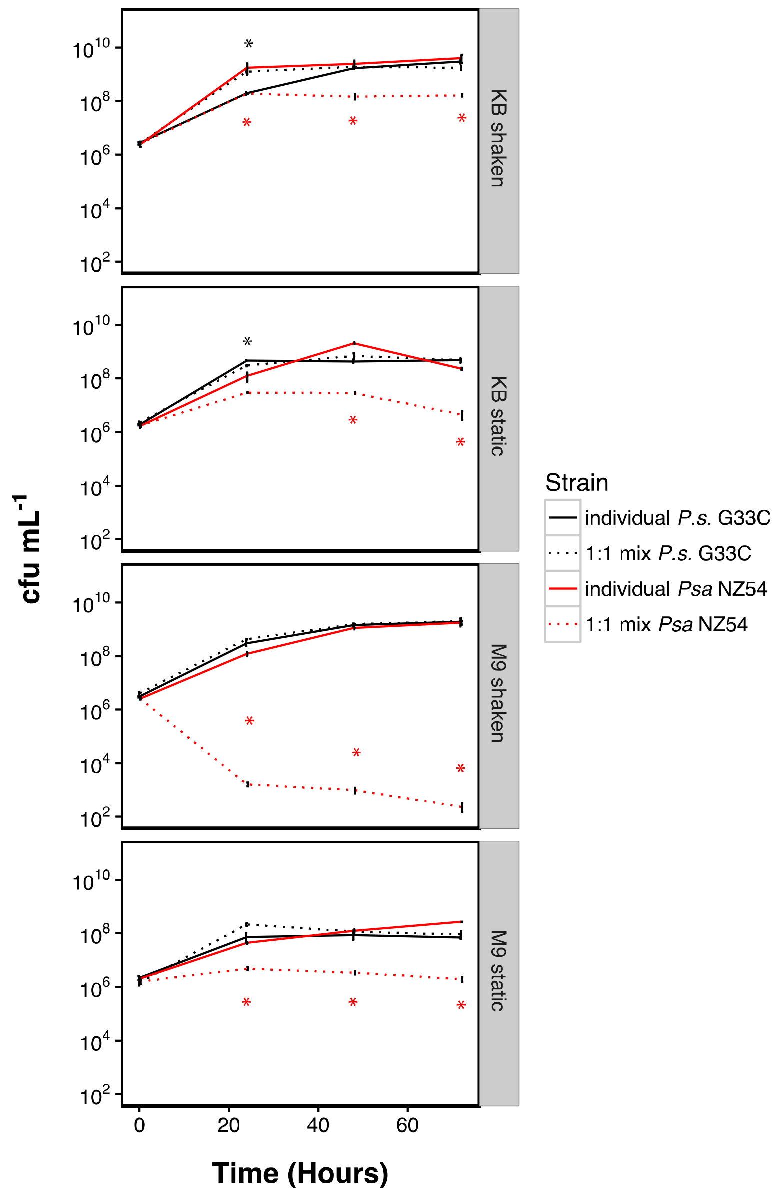

971

972 **Figure 4. Individual growth dynamics of *Psa* NZ54 and *P. syringae* G33C compared**
973 **with co-inoculation (1:1 ratio) *in vitro*.** Competition experiments were performed in
974 a 1:1 ratio (founding ratio $5x10^6$ cfu ml^{-1} each), with individual inoculations as
975 reference. Solid lines represent individual growth and dashed lines represent growth
976 in competition. The presented mean and standard error were calculated from three
977 replicates. Asterisk indicate significance between individual and co-cultured growth
978 at the 5% level (paired *t*-test).

bioRxiv preprint doi: https://doi.org/10.1101/235853; this version posted December 18, 2017. The copyright holder for this preprint (which was not certified by peer review) is the author/funder. All rights reserved. No reuse allowed without permission.

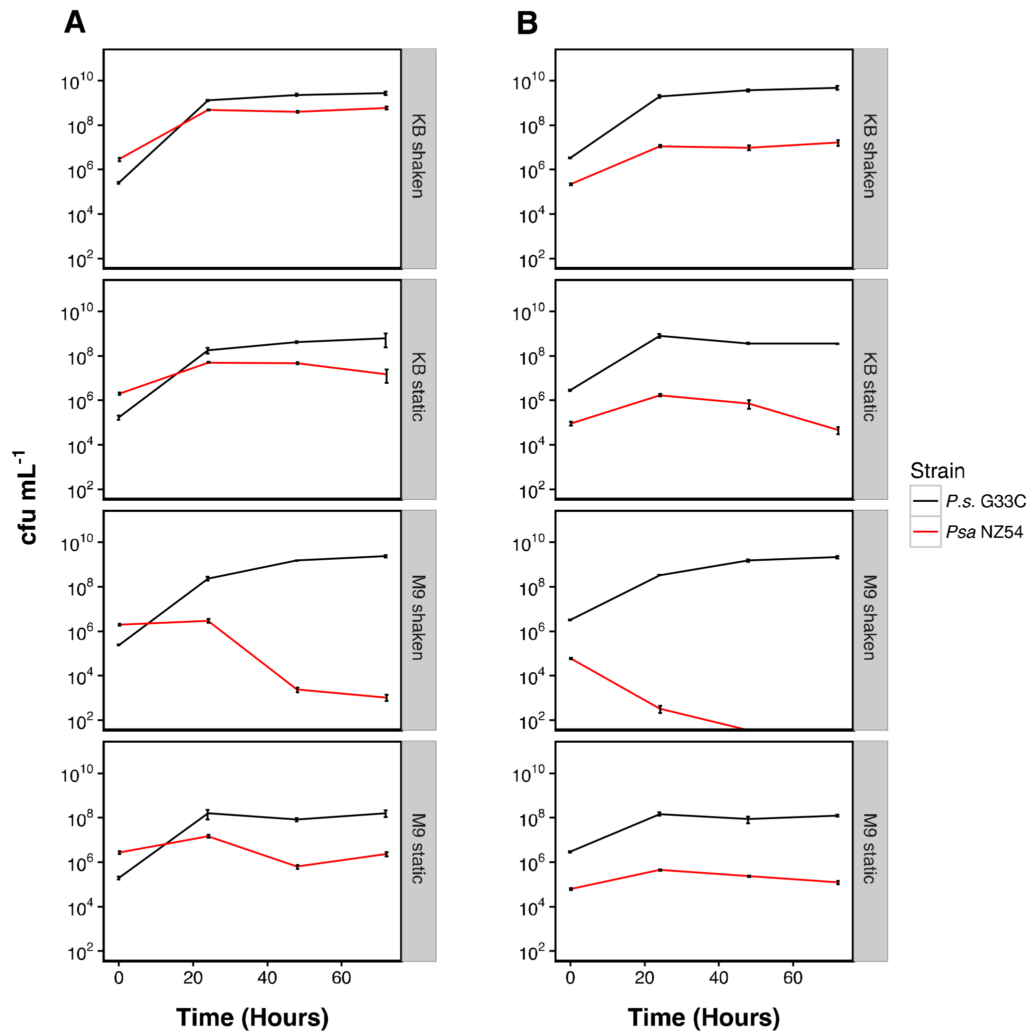

979

980 **Figure 5. *In vitro* growth curves from invasion from rare experiments for *Psa* NZ54 :**

981 ***P. syringae* G33C and vice versa.** Vials were inoculated with a (A) 10:1 ratio and (B)

982 1:10 ratio for *Psa* NZ54 : *P. syringae* G33C. The presented mean and standard error

983 were calculated from three replicates. Parameters of relative fitness of *Psa* NZ54

984 relative to *P. syringae* G33C calculated as ln difference *Psa* NZ54 – *P. syringae* G33C

985 using the Malthusian parameters at 24hrs were -2.1* ±0.02 (KB shaken), -1.9*±0.05

986 (KB static), -12.1*±0.09 (M9 shaken) and -3.9*±0.00 (M9 static). Asterisks indicate

987 significance at the 1% level (Students *t*-test).

bioRxiv preprint doi: https://doi.org/10.1101/235853; this version posted December 18, 2017. The copyright holder for this preprint (which was not certified by peer review) is the author/funder. All rights reserved. No reuse allowed without permission.

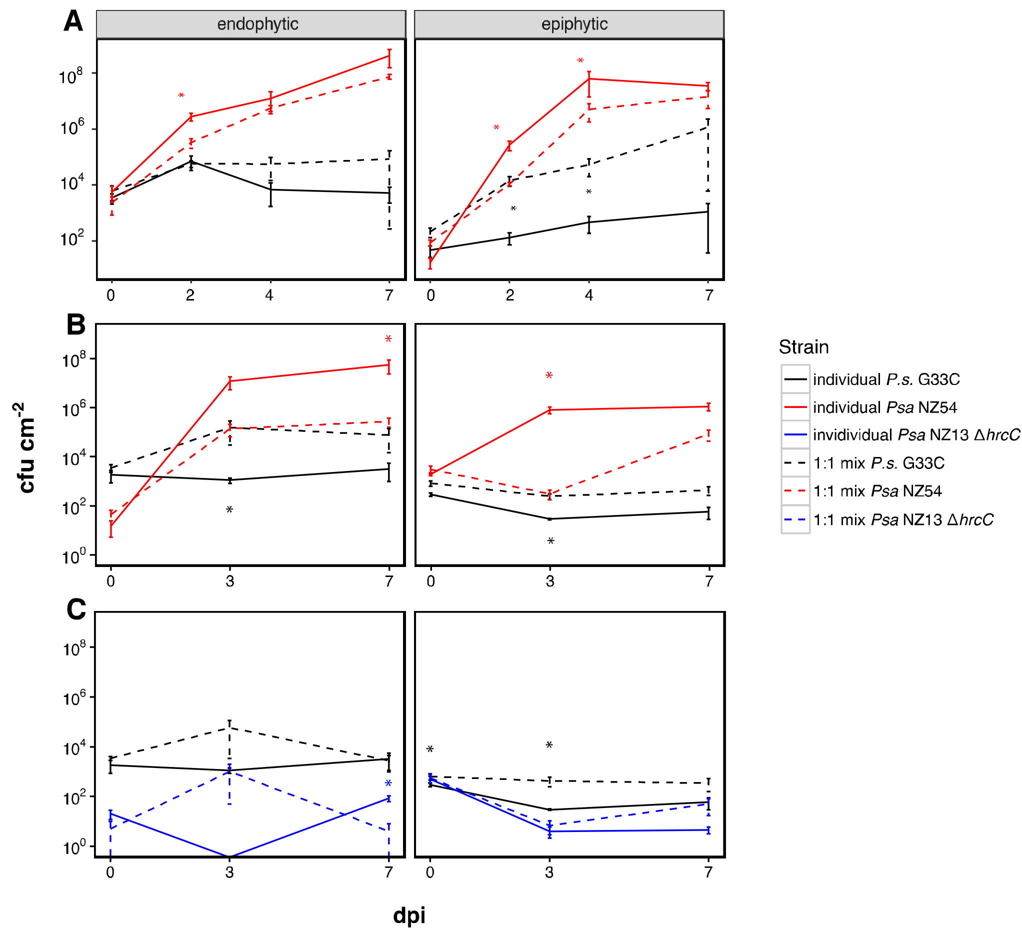

Figure 6. 1:1 competition growth assays of *Psa* NZ54 vs. *P. syringae* G33C *in planta*. 'Hort16A' plantlets (A) and 'SunGold' plantlets (B) were inoculated with a 1:1 mix of *P. syringae* G33C : *Psa* NZ54 (founding density 8x10^7 cfu ml^{-1}). (C) 'SunGold' plants were inoculated with 1:1 mix of *P. syringae* G33C : *Psa* NZ13 Δ*hrcC* (founding density 8x10^7 cfu ml^{-1}). Solid lines represent individual growth and dashed lines represent growth in competition. The presented mean and standard error were calculated from the mean of four ('Hort16A') and five ('SunGold') individual measurements. Asterisk indicate significance between individual and co-cultured growth at the 5% level (paired *t*-test).

bioRxiv preprint doi: https://doi.org/10.1101/235853; this version posted December 18, 2017. The copyright holder for this preprint (which was not certified by peer review) is the author/funder. All rights reserved. No reuse allowed without permission.

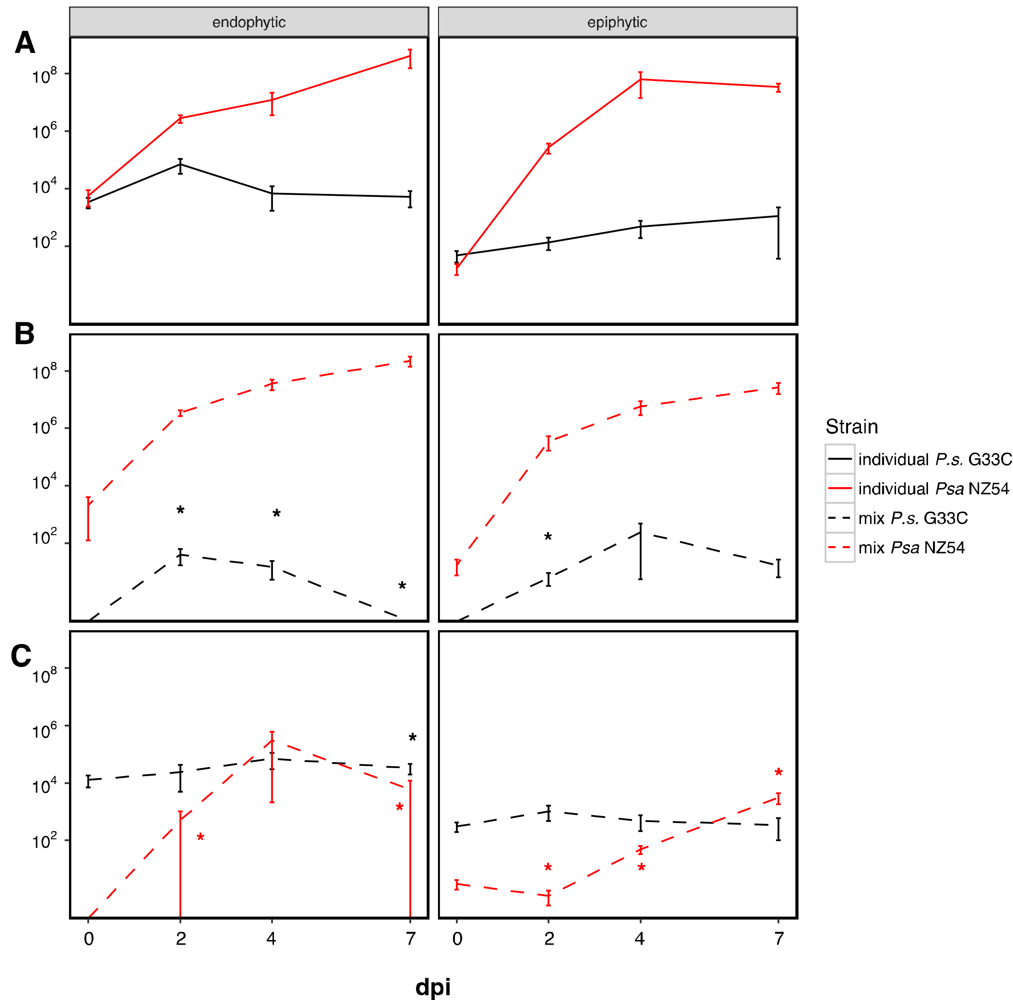

998

999 **Figure 7. Invasion from rare experiments for *Psa* NZ54 : *P. syringae* G33C *in planta.***

1000 'Hort16A' plantlets were inoculated with different ratios of strains *Psa* NZ54 : *P.*

1001 *syringae* G33C. A) Individual growth. B) Invasion from rare 100:1 and C) invasion

1002 from rare 1:100. Solid lines represent individual growth and dashed lines represent

1003 growth in competition. The presented mean and standard error were calculated

1004 from the mean of four individual measurements. Asterisks indicate significance

1005 between individual and co-cultured growth at the 5% level (paired *t*-test).

1006

bioRxiv preprint doi: https://doi.org/10.1101/235853; this version posted December 18, 2017. The copyright holder for this preprint (which was not certified by peer review) is the author/funder. All rights reserved. No reuse allowed without permission.

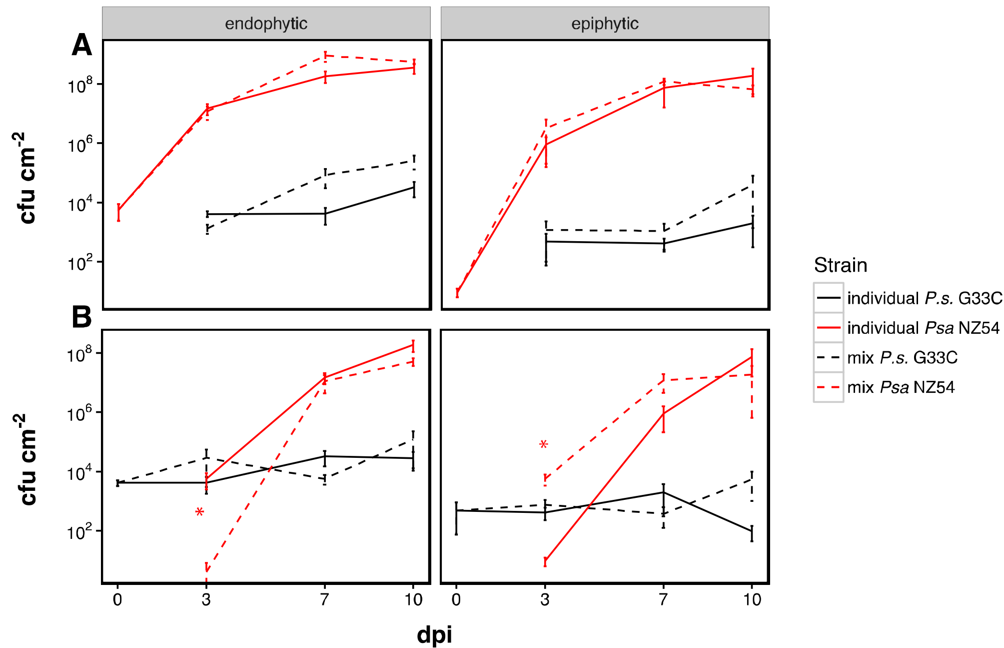

1007

1008 **Figure 8.** ***In planta*** **priority effect of** ***Psa*** **NZ54 or** ***P. syingae*** **G33C with subsequent**

1009 **inoculation of the respective second strain with the same founding density.** (A) *In*

1010 *planta* growth assay of *P. syringae* G33C using 'Hort16A' plantlets pre-inoculated for

1011 three days with *Psa* NZ54 ($8x10^7$ cfu ml^{-1}). (B) *in planta* growth assay of *Psa* NZ54

1012 using 'Hort16A' plantlets pre-inoculated for three days with *P. syringae* G33C ($8x10^7$

1013 cfu ml^{-1}). Solid lines represent individual growth and dashed lines represent growth

1014 in competition. The presented mean and standard error were calculated from the

1015 mean of five individual measurements. Asterisks indicate significance between

1016 individual and co-cultured growth at the 5% level (paired *t*-test).

bioRxiv preprint doi: https://doi.org/10.1101/235853; this version posted December 18, 2017. The copyright holder for this preprint (which was not certified by peer review) is the author/funder. All rights reserved. No reuse allowed without permission.

1017 **TABLES**

1018 **Table 1: Nucleotide and amino acid diversity.** L = length in bp, AA = amino acid, GC =
1019 average GC content in %, N_A = number of alleles, P = number of polymorphic sites,
1020 d_N/d_S ration, mut = mutations, π = nucleotide diversity indices, θ = Watterson's
1021 theta.

Locus	L (bp)	AA length	GC	N_A	P*	d_N/d_S	mut	π	θ
gapA	476	158	60.81	25	80 (16.81)	3.365	97	0.055	0.024
gyrB	507	169	53.15	28	145 (28.60)	0.018	184	0.054	0.041
gltA	529	176	58.45	27	88 (16.64)	0.011	102	0.040	0.025
rpoD	495	166	59.56	35	99 (20)	2.022	118	0.042	0.030
Mean	502	167	57.99	29	105 (20.51)	1.354	125	0.048	0.030

1022

1023 **Table 2: Average pairwise genetic diversity between and among phylogroups.**
1024 Analyses were conducted on the concatenated alignment (2006 bp, gaps removed)
1025 using the Maximum Composite Likelihood model with a gamma distribution of 1. N=
1026 number of strains.

N	Phylogroup	1	2	5	3
19	**1**	0.010			
43	**2**	0.098	0.027		
3	**5**	0.111	0.106	0.008	
83	**3**	0.099	0.063	0.107	0.014

1027
1028
1029
1030

bioRxiv preprint doi: https://doi.org/10.1101/235853; this version posted December 18, 2017. The copyright holder for this preprint (which was not certified by peer review) is the author/funder. All rights reserved. No reuse allowed without permission.

1031 **Table 3: LDhat recombination analysis.** Showing the length of the alignment in bp, N
1032 = number of sequences, mutation rate θ (=2Neμ) per site, recombination rate ρ
1033 (=2Ner) per site, ratio ε = ρ/ θ and Tajima's D.

1034

Gene	Length (bp)	N	Segregating sites	θ	ρ	ε = ρ/θ	Tajima's *D*
All *P. syringae*:							
concatenated	2010	148	335	0.030	0.006	0.187	0.513
gapA	476	148	63	0.024	0.021	0.902	2.204
gyrB	507	148	116	0.041	0.038	0.931	-0.204
gltA	529	148	74	0.025	0.012	0.461	0.678
rpoD	498	148	82	0.030	0.012	0.416	0.03
Phylogroup 1							
concat	2010	19	66	0.009	0.000	0.000	0.207
gapA	476	19	8	0.005	0.000	0.000	0.407
gyrB	507	19	20	0.011	0.000	0.000	0.611
gltA	529	19	19	0.010	0.000	0.000	0.026
rpoD	498	19	19	0.011	0.000	0.000	-0.188
Phylogroup 2							
concat	2010	43	147	0.017	0.002	0.120	1.754
gapA	476	43	29	0.014	0.006	0.457	2.307
gyrB	507	43	63	0.029	0.000	0.000	2.131
gltA	529	43	27	0.012	0.008	0.654	0.993
rpoD	498	43	28	0.013	0.023	1.734	0.621
Phylogroup 3							
concat	2010	83	163	0.016	0.015	0.937	-0.746
gapA	476	83	34	0.014	0.013	0.898	2.096
gyrB	507	83	96	0.038	0.024	0.636	-2.434
gltA	529	83	13	0.005	0.006	1.175	1.991
rpoD	498	83	20	0.008	0.033	4.073	0.3
Phylogroup 5							
concat	2010	3	23	0.008	0.000	0.000	-
gapA	476	3	-	-	-	-	-
gyrB	507	3	13	0.017	0.000	0.000	-
gltA	529	3	3	0.004	0.000	0.000	-
rpoD	498	3	7	0.009	0.000	0.000	-

1035
1036

bioRxiv preprint doi: https://doi.org/10.1101/235853; this version posted December 18, 2017. The copyright holder for this preprint (which was not certified by peer review) is the author/funder. All rights reserved. No reuse allowed without permission.

1037 **SUPPORTING FIGURES**

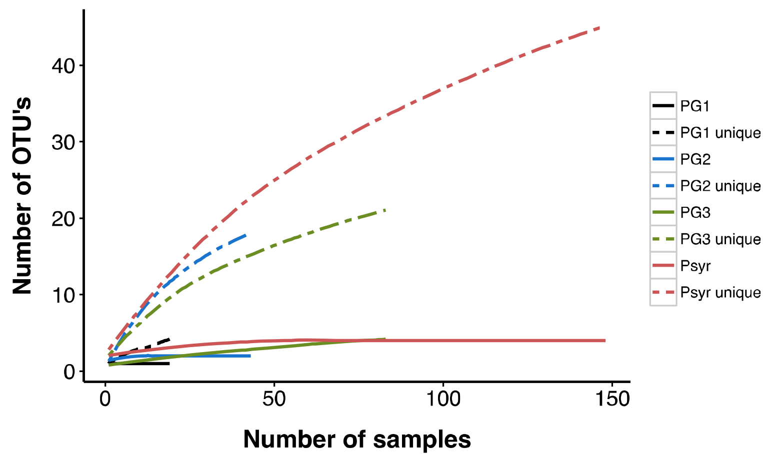

1038

1039 **Figure S1. Rarefaction curves based on the concatenated sequences.** Two curves

1040 each are shown for *P. syringae* (n=148) and the sequences grouped according to

1041 phylogroups (PG): solid lines represent grouping based on unique STs and dashed

1042 lines according to a cut-off equal to the average pairwise genetic distance of the

1043 group: PG1, PG2 & PG3 = 0.02 cut-off, Psyr all = 0.05 cut-off.

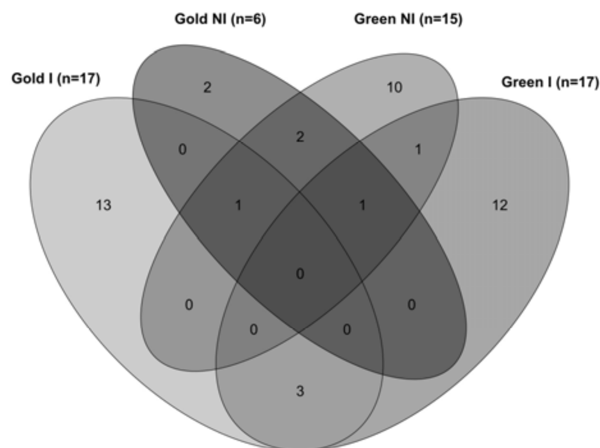

1044

1045 **Figure S2. Shared and unique STs among orchards.** Gold I = infected 'Hort16A'; Gold

1046 NI= uninfected 'Hort16A'; Green NI = uninfected 'Hayward'; Green I = infected

1047 'Hayward' orchard; n= number of STs found in orchard.

bioRxiv preprint doi: https://doi.org/10.1101/235853; this version posted December 18, 2017. The copyright holder for this preprint (which was not certified by peer review) is the author/funder. All rights reserved. No reuse allowed without permission.

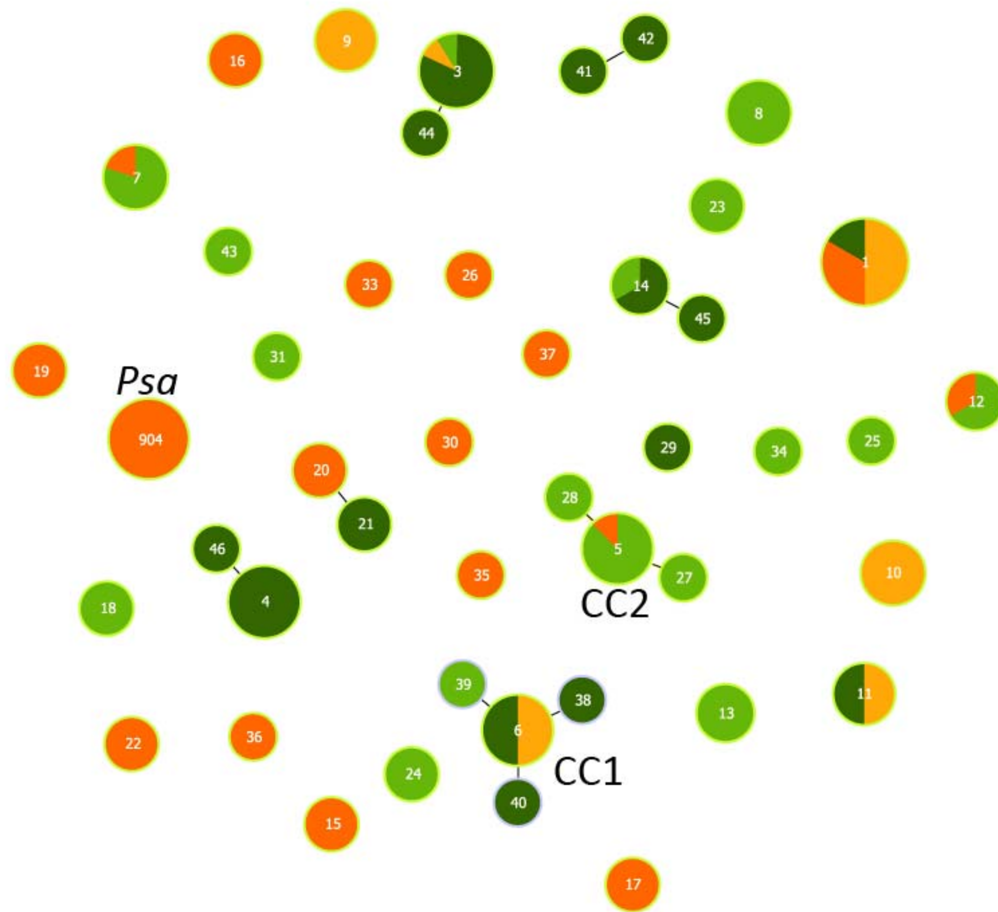

1048

1049 **Figure S3. eBurst snapshot of STs at the single locus variant level.** The size of the
1050 circles correlates with the frequency of the respective ST found in the dataset.
1051 Colours correspond to the different orchards, orange = infected 'Hort16A', yellow =
1052 uninfected 'Hort16A, dark green = infected 'Hayward', light green = uninfected
1053 'Hayward'. CC = clonal complex.

bioRxiv preprint doi: https://doi.org/10.1101/235853; this version posted December 18, 2017. The copyright holder for this preprint (which was not certified by peer review) is the author/funder. All rights reserved. No reuse allowed without permission.

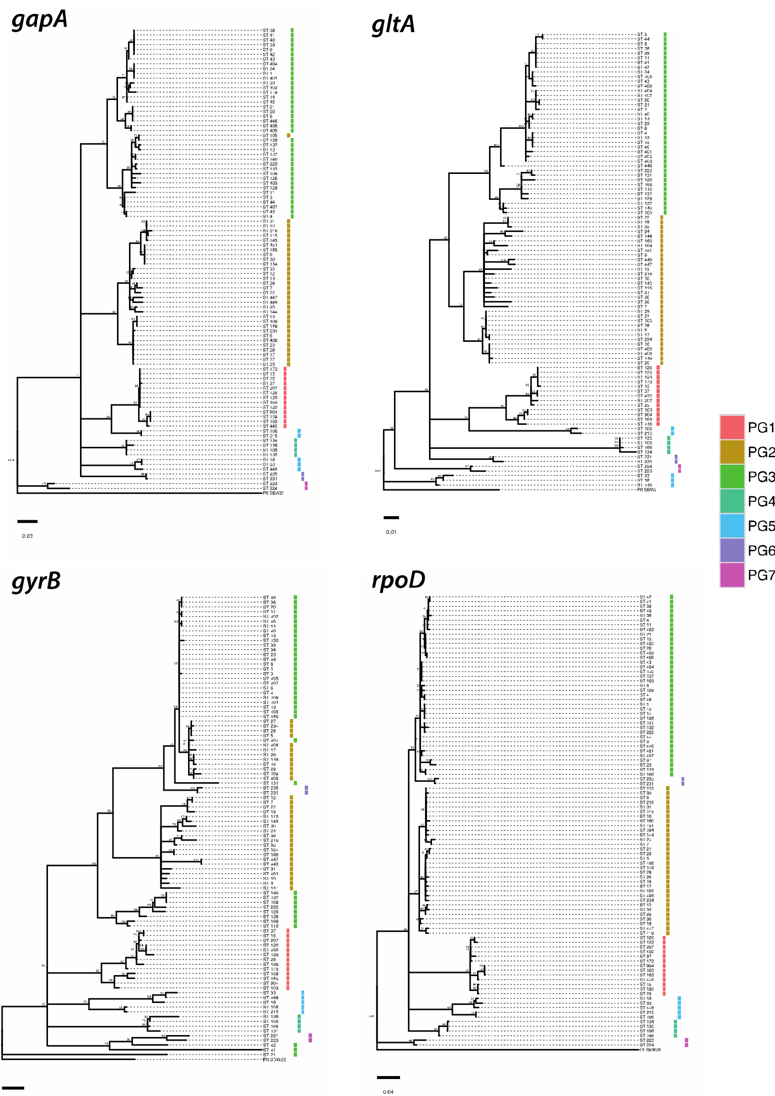

1054

1055 **Figure S4. Maximum Likelihood trees based on single genes.** Each Maximum
1056 Likelihood tree is rooted on *Pseudomonas fluorescens* SBW 25 and was
1057 reconstructed using TREEPUZZLE based on the Tamura-Nei model using 100,000
1058 puzzling steps. Trees were built using single representatives of each unique ST to
1059 improve readability of the tree. Values indicated at nodes are bootstrap values. The
1060 corresponding phylogroup distinctions based on the concatenated ML tree are
1061 indicated with the coloured squares.

bioRxiv preprint doi: https://doi.org/10.1101/235853; this version posted December 18, 2017. The copyright holder for this preprint (which was not certified by peer review) is the author/funder. All rights reserved. No reuse allowed without permission.

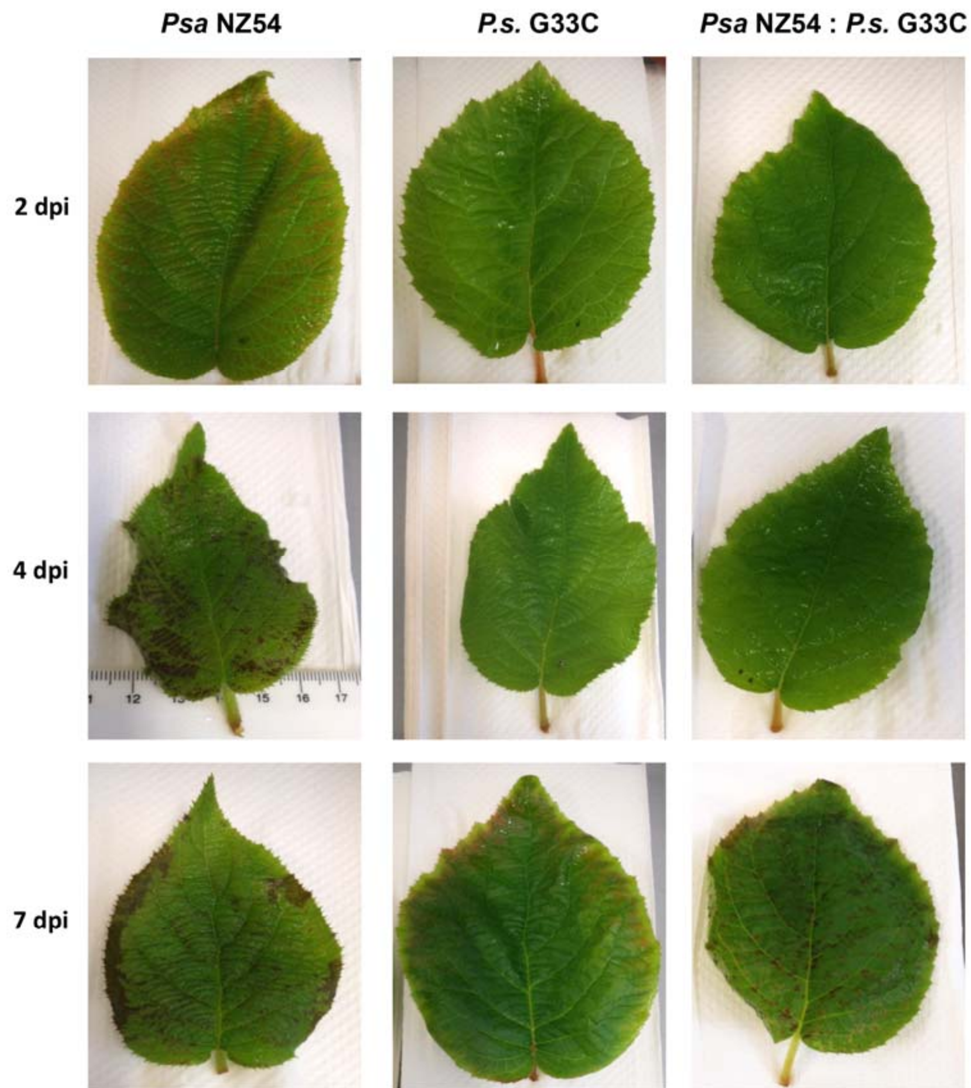

1062

1063 **Figure S5. Leaves of 'Hort16A' plants inoculated with *Psa* NZ54, *P. syringae* G33C**

1064 **and a 1:1 mix of *Psa* NZ54 : *P. syringae* G33C at 2, 4, and 7 days post inoculation.**

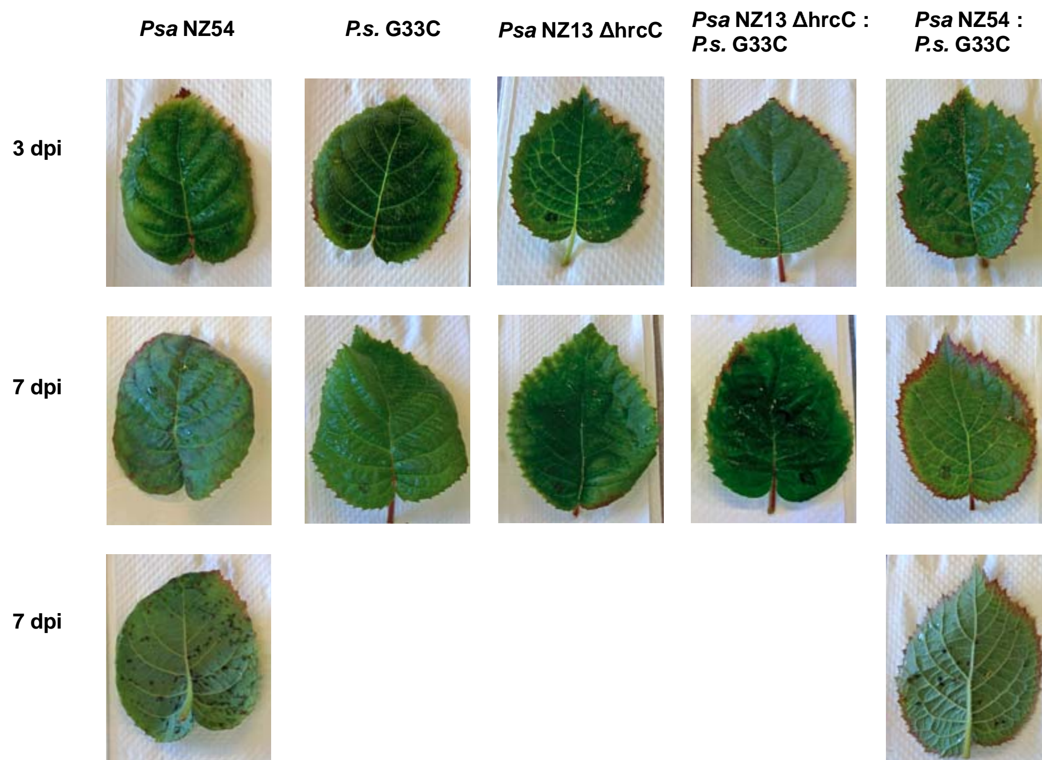

1065

1066 **Figure S6. Leaves of 'SunGold' plants inoculated with *Psa* NZ54, *P. syringae* G33C, *Psa* NZ13 ΔhrcC and 1:1 mix of the respective strain**

1067 **combinations at 3 and 7 days post inoculation.** For leaves showing minor leaf spots, the lower side of the leaf is also shown for easier

1068 detection of symptoms.

bioRxiv preprint doi: https://doi.org/10.1101/235853; this version posted December 18, 2017. The copyright holder for this preprint (which was not certified by peer review) is the author/funder. All rights reserved. No reuse allowed without permission.

bioRxiv preprint doi: https://doi.org/10.1101/235853; this version posted December 18, 2017. The copyright holder for this preprint (which was not certified by peer review) is the author/funder. All rights reserved. No reuse allowed without permission.

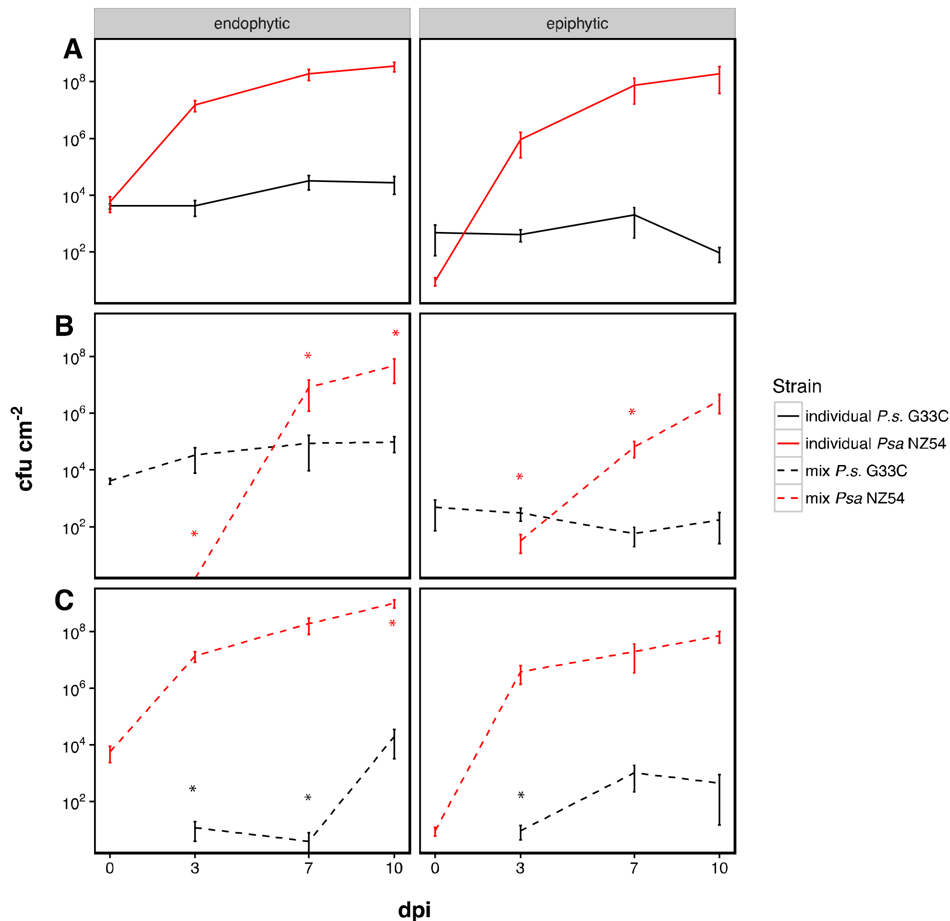

1069

1070 **Figure S7.** ***In planta*** **priority effect of** ***Psa*** **NZ54 or** ***P. syringae*** **G33C with subsequent**
1071 **inoculation of the second strain with 100-fold lower concentration.** *In planta*
1072 growth assay using 'Hort16A' plantlets pre-inoculated ($8x10^7$ cfu ml^{-1}) with one strain
1073 followed by inoculation of the second strain at ($8x10^5$ cfu ml^{-1}). The two panels
1074 display growth curves for endo- and epiphytic growth respectively. A) Individual
1075 growth, B) inoculation of *Psa* NZ 54 at day 3 and C) inoculation of *P. syringae* G33C at
1076 3 dpi. Solid lines represent individual growth and dashed lines represent growth in
1077 competition. The presented mean and standard error were calculated from the
1078 mean of five individual measurements. Asterisks indicate significance between
1079 individual and co-cultured growth at the 5% level (paired *t*-test).

bioRxiv preprint doi: https://doi.org/10.1101/235853; this version posted December 18, 2017. The copyright holder for this preprint (which was not certified by peer review) is the author/funder. All rights reserved. No reuse allowed without permission.

1080 **SUPPORTING TABLES**

1081 **Table S1. Geographic location of orchards, strain summaries and diversity indices**
1082 **per orchard.** Specification of cultivar and infection status at the time according to
1083 KVH (Kiwifruit Vine Health), orchard ID, GPS coordinates, location and month of
1084 sampling, N = number of collected *P. syringae* strains, N PG3a = number of PG3a
1085 strains in total sample, N STs = number of unique STs, N STs PG3a = number of
1086 unique STs grouping with PG3a, D = Simpsons index of diversity, D_c = converted to
1087 effective number of species, ED = Simpsons evenness.

1088 **Table S2. List of all strains.** Strain information and assigned sequence type of strains
1089 used for MLST study (all) and strains used for phylogenetic analysis (highlighted in
1090 grey). Phylogroup association only provided for isolates used for phylogenetic
1091 analysis. Alias provides the name used for competition experiments.

1092 **Table S3. PERMANOVA results of 3-factor nested analysis for differences in genetic**
1093 **diversity.**

1094 **Table S4. LDhat recombination analysis for host and disease status.** Length of
1095 alignment in bp, number of sequences, number of segregating sites, mutation rate θ,
1096 recombination rate ρ and ratio ε (ρ/ θ).

1097 **Table S5. LDhat recombination analysis for global data sorted according to**
1098 **phylogroup (PG).** Length of alignment in bp, N = number of sequences, number of
1099 segregating sites, mutation rate θ, recombination rate ρ and ratio ε (ρ/ θ).

bioRxiv preprint doi: https://doi.org/10.1101/235853; this version posted December 18, 2017. The copyright holder for this preprint (which was not certified by peer review) is the author/funder. All rights reserved. No reuse allowed without permission.

1100 **Table S6. List of primers used for construction of the deletion mutant *Psa* NZ13**

1101 **Δ*hrcC*.**

1102